Available online at www.sciencedirect.com
SCIENCE DIRECT®
Annals of Physics 317 (2005) 72–106
ANNALS of PHYSICS
www.elsevier.com/locate/aop

Decoherence in strongly coupled quantum oscillators

M.A. de Ponte, M.C. de Oliveira, M.H.Y. Moussa*

Departamento de Física, CCET, Universidade Federal de São Carlos, Via Washington Luiz Km 235, São Carlos, 13565-905, SP, Brazil

Received 12 July 2004; accepted 20 December 2004

Abstract

In this paper, we present a comprehensive analysis of the coherence phenomenon of two coupled dissipative oscillators. The action of a classical driving field on one of the oscillators is also analyzed. Master equations are derived for both regimes of weakly and strongly interacting oscillators from which interesting results arise concerning the coherence properties of the joint and the reduced system states. The strong coupling regime is required to achieve a large frequency shift of the oscillator normal modes, making it possible to explore the whole profile of the spectral density of the reservoirs. We show how the decoherence process may be controlled by shifting the normal mode frequencies to regions of small spectral density of the reservoirs. Different spectral densities of the reservoirs are considered and their effects on the decoherence process are analyzed. For oscillators with different damping rates, we show that the worse-quality system is improved and vice versa, a result which could be useful for quantum state protection. State recurrence and swap dynamics are analyzed as well as their roles in delaying the decoherence process.

PACS: 42.50.Ct; 42.50.Dv; 03.65.Bz; 32.80.−t

Keywords: Decoherence; Entanglement; Dissipation; Quantum network

* Corresponding author. Fax: +55 16 33514835.
E-mail addresses: maponte@df.ufscar.br (M.A. de Ponte), marcos@df.ufscar.br (M.C. de Oliveira), miled@df.ufscar.br (M.H.Y. Moussa).

0003-4916/$ - see front matter
doi:10.1016/j.aop.2004.12.007

1. Introduction

The process of decoherence of quantum states has long been a central issue in the description of quantum measurements [1–3]. In recent years, experimental advances in the domain of cavity QED and trapped ions have allowed the decoherence of photon [4] and phonon [5] field states to be probed in more depth, providing insights into the borderline between the classical and quantum descriptions of the physical world. The decoherence time of a superposition of coherent states in a cavity field was measured [4] and shown to be in full agreement with theoretical predictions [6,7]. In trapped ions systems, the observed damping of Rabi oscillations has motivated a number of articles on the main sources of noise leading to decoherence [8–11]. Such experimental achievements in matter–field interactions have also encouraged a deep dialog between theoretical and experimental physics, resulting in a degree of mastery of fundamental quantum phenomena that may herald a new stage in the technology of communication [12] and computation [13].

The exploration of the borderline between quantum and classical descriptions of nature [2] has impelled the generation of superposition states of mesoscopic systems, known as "Schrödinger cat states" [4,5]. Such superpositions are irreversibly affected by their surroundings, whose effect is to destroy probability interference (coherence), and continuously transformed into statistical mixtures. Thus, the environment plays a key role in the establishment of a direct correspondence between quantum and classical dynamics. While the decoherence time of a superposition state depends on the amplitude of the field, the relaxation does not, since the model adopted for the relaxation process is amplitude damping, achieved by coupling the systems bilinearly to the degrees of freedom of the reservoir.

Decoherence and its dependence upon the amplitude of the superposition state is the main obstacle to the implementation of a logic network based on quantum gates [14,15]. The dream of quantum communication and computation comes up against the nightmare of decoherence mechanisms [16], owing not only to the inevitable action of the surrounding environment but also to the intrinsic fluctuations in the interaction parameters required for logic operations [8–10]. The need for huge superpositions of qubit states in the practical implementation of logical operations imposes the requirements that the quantum systems be almost totally isolated from the environment and that the interaction parameters involved be tightly controlled. For this reason, investigation of the sources of noise in such promising quantum systems is a crucial step towards the realization of a quantum logic processor. There is also a major effort being made in present-day research, to discover mechanisms to prevent decoherence occurring in actual physical systems, by using parity kicks [17], stroboscopic feedback [18], engineered driving fields [19] or an engineered reservoir [20–22]. Moreover, quantum error correcting codes have been given which protect quantum information from any error, including gating errors, provided the error rates are below a certain threshold [23,14]. An overview of quantum error prevention strategies and a discussion of the combinations of these strategies which have recently been proposed in the literature is presented in [24]. In this light, the main concern of the present work is to analyze the

coherence dynamics and decoherence process in a network composed of two coupled dissipative oscillators, which may be field modes in dissipative cavities [25,33,34], phonon modes of trapped ions [26,27], phonon modes of surface electrons in liquid helium [28–30], etc. Master equations are derived for both weakly and strongly interacting oscillators, leading to interesting results concerning the coherence properties of the joint and the reduced system states. This work constitutes a first step towards a more comprehensive treatment of the decoherence process in multipartite quantum systems.

On attempting to extend the work on decoherence to interacting quantum oscillators coupled to distinct reservoirs, one faces the problem of deriving a master equation for different regimes of coupling between oscillators. Leaving to one side the difficulty of engineering an arbitrary coupling strength between the oscillators, in the present work we analyze not only the weak, but also the strong coupling regime, where the coupling strength between the oscillators is near the typical oscillators frequencies. In both regimes we assume that the coupling strength between the oscillators is considerably larger than the system damping rates.

In weak coupling, the coupling strength between the oscillators, labelled $\ell = 1, 2$ from here on, is considerably smaller than the typical frequencies of either oscillator, and the resulting master equation is as if the two oscillators were decoupled and a decay channel, described by the Liouville operator $\mathcal{L}_\ell \rho$, can simply be inserted into the master equation for each oscillator considered. In that case, assuming both oscillators have the same damping constant, the decoherence time for each oscillator is unaffected by the interaction with the other one. However, when the oscillators have different damping constants (field modes in cavities with different quality factors, for example), we observe that the "good-quality" oscillator gets worse, while the "bad-quality" oscillator gets better, a result which can be employed for quantum state protection.

In the strong coupling regime, we observe that a cross-decay channel $\mathcal{L}_{12}\rho$ appears, besides the usual system–reservoir individual decay channels $\mathcal{L}_\ell \rho$. This cross-decay channel modifies the decoherence process of both the joint and the reduced system state, to an extent depending crucially on the spectral density of the reservoirs. In fact, in the strong coupling regime, the normal-mode frequencies are substantially shifted from the typical oscillator frequencies, enabling us to explore the whole profile of the spectral densities of the reservoirs. We show how the decoherence process may be controlled by shifting the normal-mode frequencies to regions of small spectral density of the reservoirs. Apart from these spectral densities, the competition between the cross-decay and the usual channels can give rise to a computed delay or advance of the decoherence process, for eigenstates of the system normal modes. Note that if a system pointer variable does not commute with the operator responsible for its coupling to other system, it is clear that the internal dynamics must interfere in its decoherence time. Thus, the derivation of master equations for strongly interacting systems is a central task [31,32] in the study of decoherence in quantum networks.

It is worth mentioning some previous work concerned with coupled systems. In [25] the authors describe a proposal to achieve reversible decoherence of a

mesoscopic superposition of field states. This proposal is based on the possibility of performing a reversible coupling between two Fabry–Perot cavities. In [33], a theoretical model of the experimental proposal in [25] is given, but in [33] the inevitable coupling of the resonators to their environment is taken into account when the reversibility of coherence loss is analyzed. A system of two coupled cavities is also analyzed in [34], where just one of the cavities is interacting with a reservoir. In [34], a master equation is derived in the case of strongly coupled cavities and it is shown that the relaxation term is not simply the standard one, obtained by neglecting the interaction between the cavities. It is the aim of the present paper, in the context of cavity QED, to analyze the reversible decoherence process of [25,33], where two dissipative cavities are considered, but investigating also the regime of strongly coupled cavities, as done in [34], in which some remarkable coherence properties appear. A central result extracted from our discussion is that in a strongly interacting quantum network the decoherence time may not decrease as the number of systems considered grows. In fact, it may happen that with many coupled sites [13], as with the two coupled systems analyzed here, the decoherence time increases, depending on the spectral density of the reservoirs. For two-level systems, there is a known effect which explains this result. It is referred to as the monogamy of entanglement and is discussed in a recent work by Koashi and Winter [36]. The idea (in terms of qubits) is that a qubit which is entangled with another, cannot be completely entangled with a third qubit. The more entangled two qubits are, the less they can be entangled with another system, e.g., an environment.

Together with the strong coupling between two oscillators we consider a classical driving field feeding one of the oscillators continuously, which is intended to drive each of the coupled oscillators to a stationary coherent state [19,37], other than the vacuum state. We select a specific coupling between the oscillators, which may be responsible for the dynamics of local transfer of states or state swap between them, as discussed in [38] in relation to cavity QED with weak coupling.

The outline of this paper is as follows. In Section 2 we develop a master equation for the two coupled lossy oscillators, one of which is under the action of a classical driving field, and we analyze the weak and strong field coupling regimes. As the spectral density of the reservoirs plays a crucial role in the strong coupling regime, in Section 3 we analyze particular cases of spectral densities. In Section 4 we develop a c-number version of the master equation and solve it with reservoir temperatures set to zero. The solution of the master equation derived for strongly coupled oscillators is also analyzed in Section 4 for special initial field states. In Section 5 we discuss the recurrence and swapping dynamics of the system states. The central result of the paper, namely the coherence properties of the system states, which depend on the spectral density of the reservoir and are strongly affected by the regime of coupling, is presented in Section 6. In Section 7 we consider the two oscillators to have different damping rates and demonstrate that the coupling between them, assumed to be larger than these damping rates, makes the good-quality oscillator worse and the bad-quality oscillator better. A careful analysis of the entropy excess in our network is developed in Section 8. Finally, Section 9 concludes the paper.

2. The problem of coupled dissipative oscillators: derivation of the master equation

General results can be extracted from specific examples of quantum oscillators, such as field modes in coupled cavities [25,33,34], trapped ions [26,27], or surface electrons in liquid helium [28–30]. Let us consider a system of two interacting oscillators under the action of a driving field, as pictured in Fig. 1. We start from a positive-defined Hamiltonian so that the energy spectrum has a lower bound which is equal to zero in the absence of the driving field [39,40]. The system Hamiltonian is then given by

$$\begin{aligned} H = {} & \hbar\omega_{10}\left(a_1^\dagger + \frac{\lambda}{2\omega_{10}}a_2^\dagger\right)\left(a_1 + \frac{\lambda}{2\omega_{10}}a_2\right) + \hbar\omega_{20}\left(a_2^\dagger + \frac{\lambda}{2\omega_{20}}a_1^\dagger\right)\left(a_2 + \frac{\lambda}{2\omega_{20}}a_1\right) \\ & + \hbar\sum_k \omega_{1k}\left(b_{1k}^\dagger + \frac{V_{1k}}{\omega_{1k}}a_1^\dagger\right)\left(b_{1k} + \frac{V_{1k}}{\omega_{1k}}a_1\right) \\ & + \hbar\sum_k \omega_{2k}\left(b_{2k}^\dagger + \frac{V_{2k}}{\omega_{2k}}a_2^\dagger\right)\left(b_{2k} + \frac{V_{2k}}{\omega_{2k}}a_2\right) + \hbar F\left(\mathrm{e}^{\mathrm{i}\omega t} + a_2^\dagger\right)\left(\mathrm{e}^{-\mathrm{i}\omega t} + a_2\right), \end{aligned} \tag{1}$$

where $a_\ell^\dagger$ and a_ℓ are, respectively, the creation and annihilation operators for the oscillator mode of frequency $\omega_{\ell 0}$, whereas $b_{\ell k}$ and $b_{\ell k}^\dagger$ are the analogous operators for the kth bath mode of oscillator ℓ, whose corresponding frequency and coupling strength are $\omega_{\ell k}$ and $V_{\ell k}$, respectively. The coupling strength between the oscillators is λ and the classical driving field applied to oscillator 2 has intensity F and frequency ω. Assuming that the coupling between the oscillators and their reservoirs satisfies the condition $\sum_k (V_{\ell k})^2/\omega_{\ell k} \ll \omega_{\ell 0}$, and shifting the origin of the energy scale to $\hbar F$, we obtain from Eq. (1) the Hamiltonian $H = \sum_\ell H_\ell + H_I$, given by

$$H_\ell = \hbar\omega_\ell a_\ell^\dagger a_\ell + \hbar\sum_k \omega_{\ell k} b_{\ell k}^\dagger b_{\ell k} + \hbar\sum_k V_{\ell k}\left(a_\ell b_{\ell k}^\dagger + a_\ell^\dagger b_{\ell k}\right) + \hbar F\left(a_2^\dagger \mathrm{e}^{-\mathrm{i}\omega t} + a_2 \mathrm{e}^{\mathrm{i}\omega t}\right)\delta_{\ell 2}, \tag{2a}$$

$$H_I = \hbar\lambda\left(a_1 a_2^\dagger + a_1^\dagger a_2\right). \tag{2b}$$

Here, ω_ℓ is related to the natural frequency $\omega_{\ell 0}$ by

$$\omega_\ell = \omega_{\ell 0}\left(1 + \frac{\lambda^2}{4\omega_{10}\omega_{20}} + \delta_{\ell 2}\frac{F}{\omega_{20}}\right), \tag{3}$$

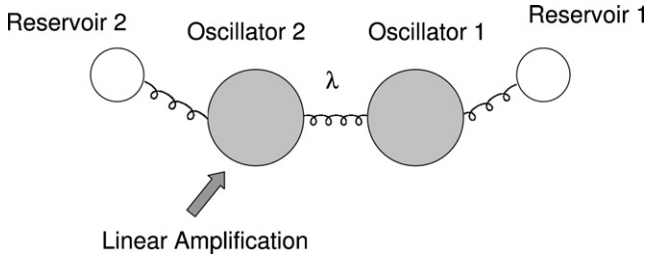

Fig. 1. Sketch of the coupled dissipative oscillators, with oscillator 2 submitted to a classical driving field.

such that in the limit of weak coupling between the oscillators ($\lambda/\omega_{\ell 0} \ll 1$) and weak amplification process ($F/\omega_{20} \ll 1$) we obtain the natural frequencies $\omega_\ell = \omega_{\ell 0}$. In this limit, we could have started from Hamiltonian H given by Eqs. (2a) and (2b) instead of (1). Note that since we are assuming weak couplings between the oscillators and their reservoirs, it is unnecessary to write these interactions in a positive-defined form, as done in Eq. (1). However, the positive-defined form for the coupling between the oscillators ensures an energy spectrum with a lower bound (equal to zero when the driving field is switched off), whatever the value of the coupling λ. Under a unitary transformation represented by the operator

$$U(t) = \exp\left[-\mathrm{i}\omega t \sum_\ell \left(a_\ell^\dagger a_\ell + \sum_k b_{\ell k}^\dagger b_{\ell k}\right)\right], \tag{4}$$

we obtain the transformed time-independent Hamiltonian

$$\mathcal{H} = U^\dagger(t) H U(t) + \mathrm{i}\frac{\mathrm{d}U^\dagger(t)}{\mathrm{d}t} U(t) = \sum_\ell \mathcal{H}_\ell + \mathcal{H}_I, \tag{5}$$

where

$$\mathcal{H}_\ell = \hbar\omega'_\ell a_\ell^\dagger a_\ell + \hbar \sum_k \omega'_{\ell k} b_{\ell k}^\dagger b_{\ell k} + \hbar\lambda\left(a_1 a_2^\dagger + a_1^\dagger a_2\right), \tag{6a}$$

$$\mathcal{H}_I = \hbar \sum_k V_{\ell k}\left(a_\ell b_{\ell k}^\dagger + a_\ell^\dagger b_{\ell k}\right) + \hbar F\left(a_2^\dagger + a_2\right), \tag{6b}$$

and the shifted frequencies are given by

$$\omega'_\ell = \omega_\ell - \omega, \tag{7a}$$

$$\omega'_{\ell k} = \omega_{\ell k} - \omega. \tag{7b}$$

From here on we consider the specific case where $\omega'_1 = \omega'_2 = \Omega$ (or $\omega_1 = \omega_2$), which links the amplitude of the driving field with the natural frequencies, as $F = (\omega_{10} - \omega_{20})[1 + \lambda^2/(4\omega_{10}\omega_{20})]$. Therefore, in the absence of the driving field, the condition $\omega'_1 = \omega'_2 = \Omega$, implies that $\omega_{10} = \omega_{20}$. With the condition $\omega'_1 = \omega'_2 = \Omega$, the Hamiltonian in Eq. (6a) can be diagonalized through the canonical transformation

$$A_1 = \frac{1}{\sqrt{2}}(a_1 + a_2), \tag{8a}$$

$$A_2 = \frac{1}{\sqrt{2}}(a_1 - a_2), \tag{8b}$$

where A_1 and A_2 satisfy the same commutation relation as a_1 and a_2: $[A_i, A_j] = 0$ and $[A_i, A_j^\dagger] = \delta_{ij}$. The purpose of these new operators is to decouple the direct interaction between oscillators 1 and 2, described by $\hbar\lambda(a_1 a_2^\dagger + a_1^\dagger a_2)$. Consequently, indirect interactions between oscillators 1 and 2 will be created through their respective reservoirs, as described by Hamiltonian $\mathbf{H} = \mathbf{H}_0 + \mathbf{H}_I$, where

$$\mathbf{H}_0 = \hbar \sum_{\ell} \left[\Omega_\ell A_\ell^\dagger A_\ell - (-1)^\ell \frac{F}{\sqrt{2}} \left(A_\ell^\dagger + A_\ell \right) + \sum_k \omega'_{\ell k} b_{\ell k}^\dagger b_{\ell k} \right], \tag{9a}$$

$$\mathbf{H}_I = \frac{\hbar}{\sqrt{2}} \sum_{\ell,k} \left[V_{1k} \left(A_\ell b_{1k}^\dagger + A_\ell^\dagger b_{1k} \right) - (-1)^\ell V_{2k} \left(A_\ell b_{2k}^\dagger + A_\ell^\dagger b_{2k} \right) \right] \tag{9b}$$

and the frequencies are given by $\Omega_\ell = \Omega - (-1)^\ell \lambda$. Without direct coupling between oscillators 1 and 2, as modelled by Hamiltonian $\mathbf{H}$, it becomes simpler to derive the master equation, following the reasoning in [7]. In the interaction picture, to the second order of perturbation, the evolution of the density matrix of the coupled oscillators is given by

$$\frac{\mathrm{d}\rho_{12}(t)}{\mathrm{d}t} = -\frac{1}{\hbar^2} \int_0^t \mathrm{d}t' \, \mathrm{Tr}_R \left[\boldsymbol{V}(t), \left[\boldsymbol{V}(t'), \rho_R(0) \otimes \rho_{12}(t) \right] \right], \tag{10}$$

where $\boldsymbol{V}(t) = \exp(\mathrm{i}\mathbf{H}_0 t/\hbar)\mathbf{H}_I \exp(-\mathrm{i}\mathbf{H}_0 t/\hbar)$. Note that the density matrix in the interaction picture, $\rho_{12}(t)$, follows from the state vector transformed by both unitary operators: $U^\dagger(t)$ defined by Eq. (4) and $\exp(\mathrm{i}\mathbf{H}_0 t/\hbar)$. Defining the operator $\mathcal{O}_\ell^\dagger(t) = \sum_k V_{\ell k} b_{\ell k}^\dagger \exp(-\mathrm{i}\omega'_{\ell k} t)/\sqrt{2}$, we proceed to obtain the master equation, assuming that the reservoir frequencies are very closely spaced, to allow a continuum summation. We have to solve the integrals appearing in Eq. (10), related to correlation functions of the form

$$\int_0^t \mathrm{d}t' \left\langle \mathcal{O}_\ell^\dagger(t) \mathcal{O}_\ell(t') \right\rangle \mathrm{e}^{-\mathrm{i}\Omega_m t + \mathrm{i}\Omega_n t'} = \int_0^t \mathrm{d}t' \int_0^\infty \frac{\mathrm{d}\omega_{\ell k}}{4\pi} V_\ell^2(\omega_{\ell k}) \sigma_\ell^2(\omega_{\ell k}) (N_\ell(\omega_{\ell k}) + 1) \times \mathrm{e}^{\mathrm{i}(\omega_{\ell k} - \Omega_n - \omega)(t - t')} \mathrm{e}^{-\mathrm{i}(\Omega_m - \Omega_n)t}, \tag{11}$$

where, from here on, $m,n = 1, 2$, the function $N_\ell(\omega_{\ell k})$ is defined by

$$\left\langle b_\ell^\dagger(\omega_{\ell k}) b_\ell(\omega_{\ell k'}) \right\rangle = 2\pi N_\ell(\omega_{\ell k}) \delta(\omega_{\ell k} - \omega_{\ell k'}) \tag{12}$$

and $\sigma_\ell(\omega_{\ell k})$ is the density of states of reservoir ℓ. Performing the variable transformations $\tau = t - t'$ and $\varepsilon = \omega_{\ell k} - \Omega_n - \omega$, we obtain, for $n = 1$ and 2, respectively,

$$\int_0^t \mathrm{d}t' \left\langle \mathcal{O}_\ell^\dagger(t) \mathcal{O}_\ell(t') \right\rangle \mathrm{e}^{-\mathrm{i}\Omega_m t + \mathrm{i}\Omega_1 t'} = \frac{1}{4\pi} \mathrm{e}^{-\mathrm{i}(\Omega_m - \Omega_1)t} \int_{-\omega_\ell^+}^\infty \mathrm{d}\varepsilon \, V_\ell^2\left(\varepsilon + \omega_\ell^+\right) \sigma_\ell^2\left(\varepsilon + \omega_\ell^+\right) \times \left[N_\ell\left(\varepsilon + \omega_\ell^+\right) + 1 \right] \int_0^t \mathrm{d}\tau \, \mathrm{e}^{\mathrm{i}\varepsilon\tau}, \tag{13a}$$

$$\int_0^t \mathrm{d}t' \left\langle \mathcal{O}_\ell^\dagger(t) \mathcal{O}_\ell(t') \right\rangle \mathrm{e}^{-\mathrm{i}\Omega_m t + \mathrm{i}\Omega_2 t'} = \frac{1}{4\pi} \mathrm{e}^{-\mathrm{i}(\Omega_m - \Omega_2)t} \int_{-\omega_\ell^-}^\infty \mathrm{d}\varepsilon \, V_\ell^2\left(\varepsilon + \omega_\ell^-\right) \sigma_\ell^2\left(\varepsilon + \omega_\ell^-\right) \times \left[N_\ell\left(\varepsilon + \omega_\ell^-\right) + 1 \right] \int_0^t \mathrm{d}\tau \, \mathrm{e}^{\mathrm{i}\varepsilon\tau}, \tag{13b}$$

where the frequency ω_ℓ has been split into two effective frequencies corresponding to the normal modes of the coupled oscillators (note that $\omega_1 = \omega_2$):

$$\omega_\ell^\pm = \omega_\ell \pm \lambda. \tag{14}$$

We have suppressed the contribution of the Cauchy principal value since it represents only a small shift in the frequency $\omega_\ell^\pm$. We note that the minimum value of ω_ℓ^- is $F[\omega_{10}/(\omega_{10}+\omega_{20})]$ which follows from $\lambda = 2\omega_{20}$. Next, we discuss both regimes: (i) the weak coupling regime $\lambda/\omega_{\ell 0} \ll 1$, and (ii) the strong coupling regime $\lambda/\omega_{\ell 0} \approx 1$. For the strong coupling regime we will assume $\lambda/\omega_{\ell 0} = 2$ to minimize ω_ℓ^-, which becomes zero when the driving field is switched off.

As usual, we consider that V_ℓ, σ_ℓ, and N_ℓ are functions that vary slowly around the frequency $\omega_\ell^\pm$, an assumption which does not apply to the function $N_\ell(\omega_\ell^-) = [\exp(\hbar\omega_\ell^-/kT) - 1]^{-1}$ (taking the reservoir to be in thermal equilibrium at temperature T) in the strong coupling regime when $F = 0$, since in this case $\omega_\ell^- \approx 0$. However, this regime (even with $F = 0$) can safely be applied to a reservoir at absolute zero, the situation we analyze in the present work. We observe that, in practice, $N_\ell(\omega_\ell^-) \approx 0$ whenever the shift in the frequency ω_ℓ^-, arising from the contribution of the Cauchy principal value, becomes sufficiently greater than $kT/\hbar$. Note that the last integrals in Eqs. (13a) and (13b) contribute significantly only when $|\varepsilon t| \lessapprox 1$, so that if we extend the upper limit of the time integration to infinity, the expressions for the correlation functions become

$$\int_0^t \mathrm{d}t' \left\langle \mathcal{O}_\ell^\dagger(t)\mathcal{O}_\ell(t')\right\rangle \mathrm{e}^{-\mathrm{i}\Omega_m t + \mathrm{i}\Omega_1 t'} = \frac{\gamma_\ell(\omega_\ell^+)}{2}\left[N_\ell(\omega_\ell^+) + 1\right]\mathrm{e}^{-\mathrm{i}(\Omega_m - \Omega_1)t}, \tag{15a}$$

$$\int_0^t \mathrm{d}t' \left\langle \mathcal{O}_\ell^\dagger(t)\mathcal{O}_\ell(t')\right\rangle \mathrm{e}^{-\mathrm{i}\Omega_m t + \mathrm{i}\Omega_2 t'} = \frac{\gamma_\ell(\omega_\ell^-)}{2}\left[N_\ell(\omega_\ell^-) + 1\right]\mathrm{e}^{-\mathrm{i}(\Omega_m - \Omega_2)t}, \tag{15b}$$

where the damping rates are defined as

$$\gamma_\ell(\omega_\ell^\pm) = \frac{1}{2}V_\ell^2(\omega_\ell^\pm)\sigma_\ell^2(\omega_\ell^\pm)\int_{-\omega_\ell^\pm}^{\infty}\mathrm{d}\varepsilon\,\delta(\varepsilon). \tag{16}$$

Defining $\Gamma_\ell = V_\ell^2(\omega_{\ell 0})\sigma_\ell^2(\omega_{\ell 0})$, in the weak coupling regime, where $\omega_\ell^\pm \approx \omega_\ell \approx \omega_{\ell 0}$, we obtain from Eq. (16) the result

$$\gamma_\ell(\omega_{\ell 0}) \approx \frac{1}{2}V_\ell^2(\omega_{\ell 0})\sigma_\ell^2(\omega_{\ell 0}) = \frac{\Gamma_\ell}{2}, \tag{17}$$

while in the strong coupling regime, where $\omega_\ell^+ \gg \omega_\ell^-$, we have

$$\gamma_\ell(\omega_\ell^+) \approx \tfrac{1}{2}V_\ell^2(\omega_\ell^+)\sigma_\ell^2(\omega_\ell^+), \tag{18a}$$

$$\gamma_\ell(\omega_\ell^-) \approx \tfrac{1}{4}V_\ell^2(\omega_\ell^-)\sigma_\ell^2(\omega_\ell^-), \quad \text{when } F = 0, \tag{18b}$$

$$\gamma_\ell(\omega_\ell^-) \approx \tfrac{1}{2}V_\ell^2(\omega_\ell^-)\sigma_\ell^2(\omega_\ell^-), \quad \text{when } F \neq 0. \tag{18c}$$

From the above results for the correlation functions, we observe that the master equation for the strong coupling regime includes that for the weak coupling regime. In fact, with $\gamma_\ell(\omega_\ell^\pm) \approx \Gamma_\ell/2$ and $N_\ell(\omega_\ell^\pm) \approx N_\ell(\omega_{\ell 0})$ we get the master equation for the weak coupling regime from that for the strong coupling regime which, described in the Schrödinger picture via the mode operators a_ℓ and $a_\ell^\dagger$, reads

$$\begin{aligned}\frac{\mathrm{d}\rho_{12}}{\mathrm{d}t} = \sum_{\ell}\Bigg\{ & \mathrm{i}\left[\rho_{12}, \Omega a_\ell^\dagger a_\ell + \lambda\sum_{m\neq\ell} a_\ell^\dagger a_m + F\left(a_2^\dagger + a_2\right)\delta_{\ell 2}\right] \\ & + \frac{F}{2\left(\Omega^2-\lambda^2\right)}\left\{\left(\Omega\delta_{\ell 1} - \lambda\delta_{\ell 2}\right)\left[\gamma_\ell\left(\omega_\ell^-\right) - \gamma_\ell\left(\omega_\ell^+\right)\right] + \left(\Omega\delta_{\ell 2} - \lambda\delta_{\ell 1}\right)\right. \\ & \left.\times\left[2\gamma_\ell(\omega) - \gamma_\ell\left(\omega_\ell^-\right) - \gamma_\ell\left(\omega_\ell^+\right)\right]\right\}\left[\rho_{12}, a_\ell - a_\ell^\dagger\right] \\ & + \frac{1}{2}\left[\gamma_\ell\left(\omega_\ell^+\right)N_\ell\left(\omega_\ell^+\right) + \gamma_\ell\left(\omega_\ell^-\right)N_\ell\left(\omega_\ell^-\right)\right]\left(\left[\left[a_\ell^\dagger, \rho_{12}\right], a_\ell\right] + \left[a_\ell^\dagger, \left[\rho_{12}, a_\ell\right]\right]\right) \\ & + \frac{1}{2}\left[\gamma_\ell\left(\omega_\ell^+\right) + \gamma_\ell\left(\omega_\ell^-\right)\right]\left(\left[a_\ell\rho_{12}, a_\ell^\dagger\right] + \left[a_\ell, \rho_{12}a_\ell^\dagger\right]\right) \\ & + \frac{1}{2}\sum_{m\neq\ell}\left[\gamma_\ell\left(\omega_\ell^+\right) - \gamma_\ell\left(\omega_\ell^-\right)\right]\left(\left[a_m\rho_{12}, a_\ell^\dagger\right] + \left[a_\ell, \rho_{12}a_m^\dagger\right]\right) \\ & + \frac{1}{2}\left[\gamma_\ell\left(\omega_\ell^+\right)N_\ell\left(\omega_\ell^+\right) - \gamma_\ell\left(\omega_\ell^-\right)N_\ell\left(\omega_\ell^-\right)\right]\left(\left[\left[a_2^\dagger, \rho_{12}\right], a_1\right] + \left[a_1^\dagger, \left[\rho_{12}, a_2\right]\right]\right)\Bigg\}. \end{aligned} \tag{19}$$

We stress that when the driving field is switched off, the second term in Eq. (19) under the summation on ℓ disappears. Otherwise, noting that $\Omega^2 - \lambda^2 = (\omega_\ell^- - \omega)(\omega_\ell^+ - \omega)$, when $F \neq 0$ and $\omega = \omega_\ell^\pm$, this term becomes

$$\frac{F}{4\lambda}\left[\gamma_\ell\left(\omega_\ell^-\right) - \gamma_\ell\left(\omega_\ell^+\right)\right]\left(\delta_{\ell 2} \mp \delta_{\ell 1}\right)\left[\rho_{12}, a_\ell - a_\ell^\dagger\right]. \tag{20}$$

Next, we derive the master equations in the weak and strong coupling regime. For simplicity, we define for the strong coupling regime $\gamma_\ell(\omega_\ell^\pm) \equiv \gamma_\ell^\pm$. Besides, we assume from here on the resonance condition for the driving field $\omega = \omega_{20}$.

2.1. Weak coupling regime

In the weak coupling regime, where $\omega_\ell^\pm \approx \omega_\ell \approx \omega_{\ell 0}$, the resonant condition for the driving field implies $\gamma_\ell(\omega) \approx \gamma_\ell^\pm \approx \Gamma_\ell/2$, so that the master equation becomes

$$\frac{\mathrm{d}\rho_{12}}{\mathrm{d}t} = \frac{\mathrm{i}}{\hbar}\left[\rho_{12}, \mathsf{H}_0\right] + \sum_{\ell}\mathcal{L}_\ell\rho_{12}, \tag{21}$$

where

$$\mathsf{H}_0 = \hbar\sum_{\ell}\left[\Omega a_\ell^\dagger a_\ell + \lambda\sum_{m\neq\ell} a_\ell^\dagger a_m + F\left(a_2^\dagger + a_2\right)\delta_{\ell 2}\right], \tag{22}$$

and the Liouville operator $\mathcal{L}_\ell\rho_{12}$ is given by the usual operator structure

$$\begin{aligned}\mathcal{L}_\ell\rho_{12} \equiv {} & \tfrac{1}{2}\Gamma_\ell\left\{N_\ell(\omega_{\ell 0})\left(\left[a_\ell^\dagger\rho_{12}, a_\ell\right] + \left[a_\ell^\dagger, \rho_{12}a_\ell\right]\right) + \left(N_\ell(\omega_{\ell 0}) + 1\right)\right. \\ & \left.\times\left(\left[a_\ell\rho_{12}, a_\ell^\dagger\right] + \left[a_\ell, \rho_{12}a_\ell^\dagger\right]\right)\right\}. \end{aligned} \tag{23}$$

Therefore, in the weak coupling regime and assuming that the driving field is resonant with oscillator 2, the interaction between the field modes and the amplification

process appears only in the von Neumann term of the master equation, and does not affect the dissipative mechanism of the individual cavities. However, when the driving field is out of resonance with oscillator 2, a correction term is added to the Liouville operator $\mathcal{L}_\ell\rho_{12}$, given by

$$\frac{F}{\left(\Omega^2-\lambda^2\right)}\left(\Omega\delta_{\ell 2}-\lambda\delta_{\ell 1}\right)\left[\gamma_\ell(\omega)-\gamma_\ell(\omega_{\ell 0})\right]\left[\rho_{12},a_\ell-a_\ell^\dagger\right]. \tag{24}$$

For a strong amplification process ($F/\omega_{20}\approx 1$), this correction becomes $F\Omega/(\Omega^2-\lambda^2)\approx 1/2$ for mode $\ell=2$, being ignored for mode $\ell=1$, since $F\lambda/(\Omega^2-\lambda^2)\ll 1$.

2.2. Strong coupling regime

Below we present the master equation for the strong coupling regime considering the general situation where both driving field and reservoir temperature are present. However, as discussed above, when switching off the driving field we must consider reservoirs at absolute zero for our results to be valid. In this regime, where $\lambda/\omega_\ell\approx 1$, the master equation is written

$$\frac{\mathrm{d}\rho_{12}}{\mathrm{d}t}=\frac{\mathrm{i}}{\hbar}\left[\rho_{12},\mathsf{H}_0\right]+\sum_\ell\mathcal{L}_\ell\rho_{12}+\mathcal{L}_{12}\rho_{12}, \tag{25}$$

where

$$\begin{aligned}\mathcal{L}_\ell\rho_{12}=&\frac{1}{2}\left(\gamma_\ell^+N_\ell\left(\omega_\ell^+\right)+\gamma_\ell^-N_\ell\left(\omega_\ell^-\right)\right)\left(\left[\left[a_\ell^\dagger,\rho_{12}\right],a_\ell\right]+\left[a_\ell^\dagger,\left[\rho_{12},a_\ell\right]\right]\right)\\&+\frac{1}{2}\left(\gamma_\ell^++\gamma_\ell^-\right)\left(\left[a_\ell\rho_{12},a_\ell^\dagger\right]+\left[a_\ell,\rho_{12}a_\ell^\dagger\right]\right)\\&+\frac{F}{2\left(\Omega^2-\lambda^2\right)}\left\{\left(\Omega\delta_{\ell 1}-\lambda\delta_{\ell 2}\right)\left(\gamma_\ell^--\gamma_\ell^+\right)+\left(\Omega\delta_{\ell 2}-\lambda\delta_{\ell 1}\right)\right.\\&\left.\times\left[2\gamma_\ell(\omega_{20})-\gamma_\ell^--\gamma_\ell^+\right]\right\}\left[\rho_{12},a_\ell-a_\ell^\dagger\right],\end{aligned} \tag{26}$$

and a cross-decay channel is included via the Liouville operator

$$\begin{aligned}\mathcal{L}_{12}\rho_{12}=&\frac{1}{2}\sum_\ell\left\{\sum_{m\neq\ell}\left(\gamma_\ell^+-\gamma_\ell^-\right)\left(\left[a_m\rho_{12},a_\ell^\dagger\right]+\left[a_\ell,\rho_{12}a_m^\dagger\right]\right)\right.\\&\left.+\left[\gamma_\ell^+N_\ell\left(\omega_\ell^+\right)-\gamma_\ell^-N_\ell\left(\omega_\ell^-\right)\right]\left(\left[\left[a_2^\dagger,\rho_{12}\right],a_1\right]+\left[a_1^\dagger,\left[\rho_{12},a_2\right]\right]\right)\right\}.\end{aligned} \tag{27}$$

Note that in the weak coupling regime, where $\gamma_\ell^\pm\approx\Gamma_\ell/2$, we obtain Eq. (21) from Eq. (25). Evidently, the Liouville operator accounting for the cross-decay channel, $\mathcal{L}_{12}\rho_{12}$, owing to the strong coupling between the oscillators, can be of the same order of magnitude as the direct-decay channels $\mathcal{L}_1\rho_{12}$ and $\mathcal{L}_2\rho_{12}$. In this regime, in contrast to the weak coupling case, a strong driving field ($F/\omega_{20}\approx 1$) modifies the Liouville operator $\mathcal{L}_\ell\rho_{12}$, such that $F\Omega/(\Omega^2-\lambda^2)$, $F\lambda/(\Omega^2-\lambda^2)\approx 1$, independently of the resonance condition. We observe that for both reservoirs at absolute zero, the

cross-decay channel is lost for the case where $\gamma_\ell^+ = \gamma_\ell^-$, which may occur, as discussed below, depending on the spectral density of the reservoirs. In what follows it will become clear that the cross-decay channel represented by the Liouville operator (27) leads to interesting results concerning the decoherence process in strongly coupled oscillators.

2.3. The split of the damping rate

It is interesting to note that for the coupled dissipative oscillators the damping rate $\gamma_\ell(\omega_{\ell 0}) = \Gamma_\ell/2$ for mode ℓ splits into γ_ℓ^+ and γ_ℓ^-. To illustrate this mechanism, we assume a Lorentzian coupling V_ℓ between the oscillators and their respective reservoirs, such that the damping function $\Gamma_\ell(\chi)$, centered on frequency χ_0, is given by

$$\Gamma_\ell(\chi) = \sigma_\ell^2 \frac{\Upsilon}{(\chi - \chi_0)^2 + \Upsilon^2}, \tag{28}$$

with the parameter Υ accounting for the spectral sharpness around the mode frequency. From the above expression and remembering, from Eq. (17), that the frequency ω_ℓ splits into two shifted frequencies $\omega_\ell^\pm$, we obtain the double Lorentzian function depicted in Fig. 2

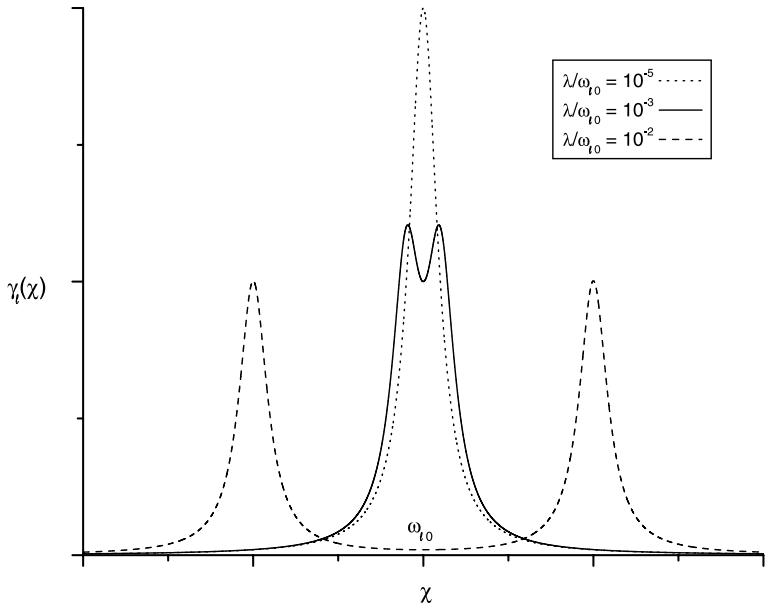

Fig. 2. Damping function $\gamma_\ell(\chi)$ assuming a Lorentzian coupling V_ℓ between oscillator ℓ and its respective reservoir. In the weak coupling regime the function $\gamma_\ell(\chi)$ is centered around ω_ℓ (dotted line). As λ increases, the damping function splits into two Lorentzian functions whose peak heights are half the original value Γ_ℓ (solid line). On the way to the strong coupling regime the two peaks can be clearly distinguished as shown by the dashed line.

$$\Gamma_\ell(\chi) = \frac{\Upsilon\sigma_\ell^2}{2}\left(\frac{1}{(\chi-\omega_\ell^+)^2+\Upsilon^2}+\frac{1}{(\chi-\omega_\ell^-)^2+\Upsilon^2}\right) = \gamma_\ell(\omega_\ell^+)+\gamma_\ell(\omega_\ell^-), \qquad (29)$$

with maxima on $\omega_\ell^\pm$. In fact, from master equation (19), we observe that in the weak coupling regime, when $\gamma_\ell(\omega_\ell^+)+\gamma_\ell(\omega_\ell^-) = \Gamma_\ell(\omega_{\ell 0}) = \Gamma_\ell$ (since $\gamma_\ell(\omega_\ell^+) = \gamma_\ell(\omega_\ell^-) = \Gamma_\ell/2$), we obtain the expected Liouville form for two independent dissipative oscillators. From Eq. (29) it is immediately obvious that in the weak coupling regime, where $\omega_\ell^\pm \approx \omega_{\ell 0}$, the damping function presents only one peak, shown by the dotted line in Fig. 2. In this regime, the damping rate, assumed to be the maximum of a sharp-peaked damping function, i.e., Γ_ℓ (for a small value of Υ), becomes twice the value designated for $\gamma_\ell(\omega_\ell^\pm)$. As $\lambda = \pm(\omega_\ell^\pm - \omega_\ell)$ increases, the damping function splits into two Lorentzian functions whose peak heights are half the original value Γ_ℓ, as dictated by the master equation (25) and shown by the solid line in Fig. 2. The dashed line shows the situation where the two peaks can be clearly distinguished, on the way to the strong coupling regime, $\lambda/\omega_{\ell 0} \approx 1$, where the peak centered on ω_ℓ^- shifts to around the value $F[\omega_{10}/(\omega_{10}+\omega_{20})]$, which can be made as smaller as we wish by decreasing the amplitude of the driving field. In practice, the effect of the strong coupling between the oscillators is essentially to shift the normal-mode frequency $\omega_\ell^\pm$ to regions far way from the natural frequency of the oscillator $\omega_{\ell 0}$, where the spectral density of the reservoir may be significantly different from that around $\omega_{\ell 0}$. In this connection, the spectral density of the reservoir $\sigma_\ell(\omega_{\ell k})$ plays a crucial role in the dissipative dynamics of strongly coupled oscillators, since the magnitude of the damping rate $\gamma_\ell(\omega_\ell)$ depends on $\sigma_\ell(\omega_\ell)$. For this reason, we next analyze reservoirs with different spectral densities to illustrate the interesting features arising from the strong coupling regime. Evidently, the physical systems under consideration and their dissipative mechanisms (i.e., the nature of the reservoirs and their spectral densities), will be decisive for our analysis.

We finally stress that coupled classical oscillators give rise to mode splitting and that, in general, different damping rates are associated to each of these modes. For trapped ions, the fact that the stretching mode is less affected by damping than the center-of-mass mode was explicitly demonstrated experimentally in [41].

3. Spectral densities of the reservoirs

It is possible that specific spectral densities could be achieved through engineered reservoirs, a program which has recently attracted considerable attention also in attempts to control the decoherence process of quantum states [20–22]. Therefore, the results we present below, depending crucially on the spectral density of the reservoir, might provide a motivation for future theoretical proposals on engineered reservoirs. For the following discussion we consider the strong coupling regime and set both driving field and reservoir temperatures to zero ($F, T = 0$) and remember, from the definition $\gamma_\ell(\omega_\ell^\pm) \equiv \gamma_\ell^\pm$, that the parameter $\gamma_\ell^\pm$ depends on the reservoir spectral density around $\omega_\ell^\pm$.

3.1. Markovian white noise

We start with the simplest case of Markovian white noise, where the spectral density of the reservoir is invariant over translation in frequency space, as depicted in Fig. 3A. In this case, assuming a Lorentzian coupling between the oscillators and their respective reservoirs, centered around the effective frequencies $\omega_\ell^\pm$, as in Eq. (29), we get $\gamma_\ell^- = \gamma_\ell^+/2 = \Gamma_\ell/4$. In fact, the effective frequency ω_ℓ^- shifts to around zero (when $F = 0$), and so, the system–reservoir coupling γ_ℓ^- becomes half the value $\gamma_\ell^+ = \Gamma_\ell/2$, as can be concluded immediately from Eqs. (18a)–(18c). The system–reservoir couplings around $\omega_\ell^\pm$ are represented by shaded regions in Fig. 3A. Therefore, for a Markovian white noise reservoir, strong coupling between the oscillators delays the decoherence time of a joint state which is an eigenstate of normal mode ω_ℓ^-, as will be discussed latter. Next, we analyze two cases of non-Markovian colored noise, still assuming that V_ℓ, σ_ℓ, and N_ℓ are functions that vary slowly around the frequency $\omega_\ell^\pm$, as discussed above.

3.2. A Lorentzian spectral density

Let us consider a Lorentzian spectral density of the reservoir which goes to zero at both effective frequencies ω_ℓ^- and ω_ℓ^+ (Fig. 3B). The achievement of a reservoir spectral density for which $\sigma_\ell(\omega_\ell^\pm) \approx 0$ would result in a damping function $\gamma_\ell(\omega_\ell^\pm)$ arising from both terms on the right hand side of Eq. (29) (i.e.,

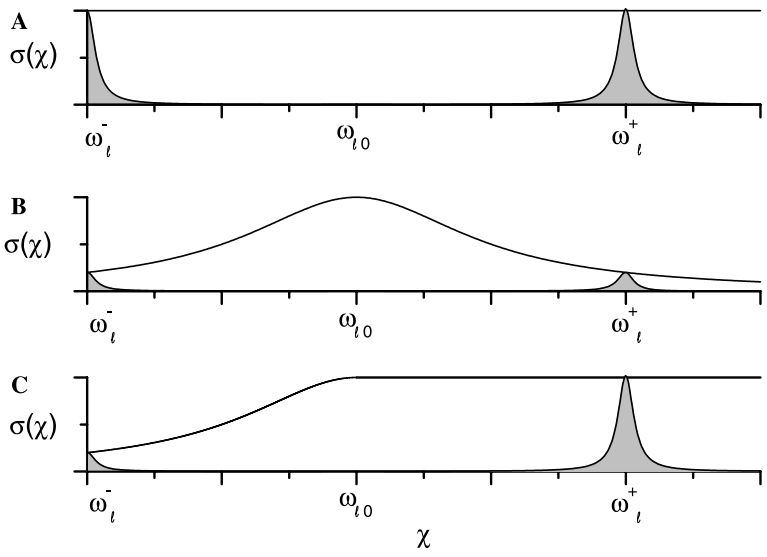

Fig. 3. Spectral density of the reservoir $\sigma_\ell(\chi)$ for (A) Markovian white noise, (B) a Lorentzian spectral density, and (C) a wide Lorentzian spectral density. The system–reservoir couplings around $\omega_\ell^\pm$ are represent by the shaded regions.

$\Upsilon\sigma_\ell^2/[(\chi-\omega_\ell^{\pm})^2+\Upsilon^2]\approx 0$), neither of which would contribute significantly to the relaxation process. Therefore, for such a Lorentzian coupling between the field modes and their respective reservoirs, we get from Eqs. (18a), (18b), and (18c) the rates $\gamma_\ell^{\pm}\ll\Gamma_\ell$, since both effective frequencies ω_ℓ^+ and ω_ℓ^- shift to regions where the spectral densities of the reservoir are considerable smaller than that around $\omega_{\ell 0}$. In view of the difficulty of obtaining a Lorentzian spectral density sufficiently small around ω_ℓ^+, such that $\sigma_\ell(\omega_\ell^+)\approx 0$, we next turn to a more realistic case, which we call a wide Lorentzian spectral density.

3.3. A wide Lorentzian spectral density

Finally, we consider a wide Lorentzian spectral density, which goes to zero at the effective frequency ω_ℓ^-, reaches a flat maximum around $\omega_{\ell 0}$, continues on it up to around ω_ℓ^+ and only reaches zero again at frequencies far beyond ω_ℓ^+, as depicted in Fig. 3C. Differently from the Lorentzian spectral density, in this case only the damping function γ_ℓ^- arising from the second term on the right hand side of Eq. (29) (i.e., $\Upsilon\sigma_\ell^2/[(\chi-\omega_\ell^-)^2+\Upsilon^2]\approx 0$) does not contribute significantly to the relaxation process; i.e., $\gamma_\ell^-\ll\Gamma_\ell$, since the resonances around the effective frequency ω_ℓ^- can be disregarded. Only the system–reservoir coupling around the effective frequency ω_ℓ^+ contributes to the relaxation process of this mode ($\gamma_\ell^+=\Gamma_\ell/2$). Such a model can be considered as similar to subhomic dissipation [3,42] and can be reasonably applied for a variety of phonon-like spectral densities where the de Debye model applies very well in the domain of small frequencies.

4. The Fokker–Planck equation

Using the standard procedures, we derive a c-number version of the master equation (19) for the Glauber–Sudarshan P-representation [43,44,7,45] given by

$$\frac{\mathrm{d}P}{\mathrm{d}t}=\frac{1}{2}\sum_{\ell,m}\left[\Pi_\ell+C_\ell(\alpha_1,\alpha_2)\frac{\partial}{\partial\alpha_\ell}+D_{\ell m}\frac{\partial^2}{\partial\alpha_\ell\partial\alpha_m^*}+\text{H.c.}\right]P, \tag{30}$$

where the function $C_\ell(\alpha_1,\alpha_2)$ and the matrix elements $D_{\ell m}$ satisfy

$$C_\ell(\alpha_1,\alpha_2)=B_\ell+\alpha_\ell E_\ell^+ +\alpha_{\ell-(-1)^\ell}E_\ell^-, \tag{31a}$$

$$D_{\ell\ell}=\gamma_\ell^+ N_\ell\big(\omega_\ell^+\big)+\gamma_\ell^- N_\ell\big(\omega_\ell^-\big), \tag{31b}$$

$$D_{12}=D_{21}=\frac{1}{2}\sum_\ell\left[\gamma_\ell^+ N_\ell\big(\omega_\ell^+\big)-\gamma_\ell^- N_\ell\big(\omega_\ell^-\big)\right], \tag{31c}$$

while the parameters Π_ℓ, $E_\ell^{\pm}$, and B_ℓ are defined by

$$\Pi_\ell=\tfrac{1}{2}\big(\gamma_\ell^-+\gamma_\ell^+\big), \tag{32}$$

$$E_\ell^+=\tfrac{1}{2}\big(\gamma_\ell^++\gamma_\ell^-+2\mathrm{i}\Omega\big), \tag{33}$$

$$E_\ell^- = \tfrac{1}{2}\left(\gamma_\ell^+ - \gamma_\ell^- + 2\mathrm{i}\lambda\right), \tag{34}$$

$$B_\ell = \mathrm{i}F\delta_{\ell 2} - \frac{F}{2\left(\Omega^2 - \lambda^2\right)}\left[(\Omega\delta_{\ell 2} - \lambda\delta_{\ell 1})\left(2\gamma_\ell(\omega_{20}) - \gamma_\ell^- - \gamma_\ell^+\right) + (\Omega\delta_{\ell 1} - \lambda\delta_{\ell 2})\left(\gamma_\ell^- - \gamma_\ell^+\right)\right]. \tag{35}$$

Note that the drift coefficient C_ℓ is linearly dependent upon both variables α_1 and α_2, while the diffusion coefficient D_{mn} is constant, determining an Orstein–Uhlenbeck process [46].

In an extreme case of the weak coupling regime, which we do not consider in the present work, where $\lambda \lesssim \Gamma_\ell$, the drift coefficient C_ℓ depends mainly on α_ℓ and the diffusion coefficient is given by $D_{mn} = \delta_{mn}\mathrm{D}_{mm}$, which is strictly positive. In this particular case, the dynamics of the two oscillators decouple, since the two-mode state relaxes, due to the damping process, before they have time to interact. Thus

$$\frac{\mathrm{d}P}{\mathrm{d}t} = \sum_\ell \left[\Pi_\ell + C_\ell(\alpha_\ell)\frac{\partial}{\partial\alpha_\ell} + \frac{D_{\ell\ell}}{2}\frac{\partial^2}{\partial\alpha_\ell\partial\alpha_\ell^*} + \mathrm{H.c.}\right]P, \tag{36}$$

and the general solution is simply the summation of the independent solutions for each mode.

4.1. Solution of the Fokker–Planck equation at absolute zero

From now on we assume both reservoirs set to absolute zero, such that $N_\ell(\omega_\ell^\pm) = 0$. This assumption is equivalent to setting $D_{mn} = 0$, and thus the Fokker–Planck equation (30) reduces to a simple drift equation

$$\frac{\mathrm{d}P}{\mathrm{d}t} = \sum_\ell \left[\Pi_\ell + C_\ell(\alpha_1, \alpha_2)\frac{\partial}{\partial\alpha_\ell} + \mathrm{H.c.}\right]P. \tag{37}$$

With the substitution $P = P'\exp[2(\Pi_1 + \Pi_2)t]$, we simplify the above equation to the form

$$\frac{\mathrm{d}P'}{\mathrm{d}t} = \sum_\ell \left[C_\ell(\alpha_1, \alpha_2)\frac{\partial}{\partial\alpha_\ell} + \mathrm{H.c.}\right]P', \tag{38}$$

and assuming that $P'(\alpha_1, \alpha_2, t) = P'(\alpha_1(t), \alpha_2(t))$, we get

$$\frac{\mathrm{d}}{\mathrm{d}t}P'(\alpha_1(t), \alpha_2(t)) = \sum_\ell \left(\frac{\partial\alpha_\ell}{\partial t}\frac{\partial}{\partial\alpha_\ell} + H.c\right)P'(\alpha_1(t), \alpha_2(t)). \tag{39}$$

Therefore, from Eqs. (38) and (39) we obtain the system of coupled equations

$$\frac{\partial\alpha_1}{\partial t} = B_1 + \alpha_1 E_1^+ + \alpha_2 E_1^-, \tag{40a}$$

$$\frac{\partial\alpha_2}{\partial t} = B_2 + \alpha_2 E_2^+ + \alpha_1 E_2^-, \tag{40b}$$

which leads to

$$\frac{\partial^2\alpha_1}{\partial t^2} - \left(E_1^+ + E_2^+\right)\frac{\partial\alpha_1}{\partial t} + \alpha_1\left(E_1^+E_2^+ - E_1^-E_2^-\right) + \left(B_1E_2^+ - B_2E_1^-\right) = 0. \tag{41}$$

Next, we define the parameters (where we have disregarded terms of order $O^2(\gamma_\ell^\pm/\lambda)$) $\Lambda = (\gamma_1^+ + \gamma_2^+ + \gamma_1^- + \gamma_2^-)/4 + i\Omega$, $\Delta = (\gamma_1^+ - \gamma_2^+ + \gamma_1^- - \gamma_2^-)/4$, $\Phi = (\gamma_1^+ + \gamma_2^+ - \gamma_1^- - \gamma_2^-)/4$, $\Theta = (\gamma_1^+ - \gamma_2^+ - \gamma_1^- + \gamma_2^-)/4$, and the time-dependent functions.

$$W^\pm = \cosh\Phi t\left(\cos\lambda t \pm \frac{\Delta}{\lambda}\sin\lambda t\right) + i\sinh\Phi t\left(\sin\lambda t \mp \frac{\Delta}{\lambda}\cos\lambda t\right), \tag{42a}$$

$$Z^\pm = \left(\sinh\Phi t\cos\lambda t \pm \frac{\Theta}{\lambda}\cosh\Phi t\sin\lambda t\right) + i\left(\cosh\Phi t\sin\lambda t \mp \frac{\Theta}{\lambda}\sinh\Phi t\cos\lambda t\right). \tag{42b}$$

Defining also the parameters

$$G_1 = \frac{B_2E_1^- - B_1E_2^+}{E_1^+E_2^+ - E_1^-E_2^-}, \tag{43}$$

$$G_2 = \frac{B_1E_2^- - B_2E_1^+}{E_1^+E_2^+ - E_1^-E_2^-}, \tag{44}$$

we finally obtain the solution of Eqs. (40a and 40b), written in the compact form

$$\alpha_1(t) = e^{\Lambda t}\left[\left(\alpha_1^0 - G_1\right)W^+ + \left(\alpha_2^0 - G_2\right)Z^+\right] + G_1, \tag{45a}$$

$$\alpha_2(t) = e^{\Lambda t}\left[\left(\alpha_2^0 - G_2\right)W^- + \left(\alpha_1^0 - G_1\right)Z^-\right] + G_2, \tag{45b}$$

where α_ℓ^0 indicates $\alpha_\ell(t=0)$. From the solution of Eqs. (45a) and (45b) it follows that the Fokker–Planck equation (37) can be solved to give

$$P(\alpha_1,\alpha_2,t) = e^{2(\Pi_1+\Pi_2)t}P(\alpha_1,\alpha_2,0)|_{\alpha_\ell\to\alpha_\ell(t)}, \tag{46}$$

where $P(\alpha_1, \alpha_2, 0)$ is the P-function for the initial state. The evolved P-function is then obtained by simply replacing α_ℓ by the evolved parameters given by Eqs. (45a) and (45b). Finally, from Eq. (46) the evolved density operator related to (19) follows from

$$\rho_{12}(t) = \int d^2\alpha_1 d^2\alpha_2 P(\alpha_1,\alpha_2,t)|\alpha_1,\alpha_2\rangle\langle\alpha_1,\alpha_2|. \tag{47}$$

4.2. Initial joint states

Next, we obtain the density operator $\rho_{12}(t)$ supposing that the modes 1 and 2 are prepared in a superposition of coherent states of the form

$$|\varphi\rangle = \mathcal{N}_\pm\left(\left|\beta_I^1,\beta_I^2\right\rangle \pm \left|\beta_{II}^1,\beta_{II}^2\right\rangle\right), \tag{48}$$

where $\mathcal{N}_{\pm}$ stands for the normalization factor and the subscripts I, II are related to different coherent states participating in the superposition. From Eqs. (47) and (48), the corresponding evolved density operator is given by

$$\rho_{12}(t) = \sum_{m,n=I,II} C_{mn}(t)|\varsigma_m, \zeta_m\rangle\langle\varsigma_n, \zeta_n|, \tag{49}$$

where the labels ς and ζ represent the states of modes 1 and 2, respectively. The expansion coefficients read

$$\begin{aligned} C_{mn}(t) = {} & \mathcal{N}_{\pm}^2(\pm 1)^{1-\delta_{mn}} \left\langle \beta_n^1 \middle| \beta_m^1 \right\rangle^{1-\exp(-2\mathrm{Re}\{\Lambda\}t)\left(|W^-|^2+|Z^-|^2\right)} \\ & \times \left\langle \beta_n^2 \middle| \beta_m^2 \right\rangle^{1-\exp(-2\mathrm{Re}\{\Lambda\}t)\left(|W^+|^2+|Z^+|^2\right)} \mathrm{e}^{\mathrm{i}(\theta_{mn}^{(1)}+\theta_{mn}^{(3)})+\theta_{mn}^{(2)}+\theta_{mn}^{(4)}}, \end{aligned} \tag{50}$$

while the states ς and ζ are given by

$$\varsigma_\ell = \mathrm{e}^{-\Lambda t}\left[\left(\beta_\ell^1 - G_1\right)W^- - \left(\beta_\ell^2 - G_2\right)Z^+\right] + G_1, \tag{51a}$$

$$\zeta_\ell = \mathrm{e}^{-\Lambda t}\left[\left(\beta_\ell^2 - G_2\right)W^+ - \left(\beta_\ell^1 - G_1\right)Z^-\right] + G_2. \tag{51b}$$

We define the time-dependent functions

$$\begin{aligned} \theta_{mn}^{(1)} = {} & \mathrm{Im}\left\{\mathrm{e}^{-\Lambda^* t}\left[(W^+)^*\left(\beta_m^{2*} - \beta_n^{2*}\right) - (Z^-)^*\left(\beta_m^{1*} - \beta_n^{1*}\right)\right]\right. \\ & \left.\times\left[\mathrm{e}^{-\Lambda t}(G_1 Z^- - G_2 W^+) + G_2\right]\right\}, \end{aligned} \tag{52a}$$

$$\begin{aligned} 2\theta_{mn}^{(2)} = {} & \mathrm{e}^{-2\mathrm{Re}\{\Lambda\}t}\left\{W^+(Z^-)^*\left[\beta_n^{1*}\left(\beta_m^2 - \beta_n^2\right) - \left(\beta_m^{1*} - \beta_n^{1*}\right)\beta_m^2\right]\right. \\ & \left.-(W^+)^* Z^-\left[\beta_m^1\left(\beta_m^{2*} - \beta_n^{2*}\right) - \left(\beta_m^1 - \beta_n^1\right)\beta_n^{2*}\right]\right\}, \end{aligned} \tag{52b}$$

$$\begin{aligned} \theta_{mn}^{(3)} = {} & \mathrm{Im}\left\{\mathrm{e}^{-\Lambda^* t}\left[(W^-)^*\left(\beta_m^{1*} - \beta_n^{1*}\right) - (Z^+)^*\left(\beta_m^{2*} - \beta_n^{2*}\right)\right]\right. \\ & \left.\times\left[\mathrm{e}^{-\Lambda t}(G_2 Z^+ - G_1 W^-) + G_1\right]\right\}, \end{aligned} \tag{52c}$$

$$\begin{aligned} 2\theta_{mn}^{(4)} = {} & \mathrm{e}^{-2\mathrm{Re}\{\Lambda\}t}\left\{W^-(Z^+)^*\left[\left(\beta_m^1 - \beta_n^1\right)\beta_n^{2*} - \beta_m^1\left(\beta_m^{2*} - \beta_n^{2*}\right)\right]\right. \\ & \left.-(W^-)^* Z^+\left[\left(\beta_m^{1*} - \beta_n^{1*}\right)\beta_m^2 - \beta_n^{1*}\left(\beta_m^2 - \beta_n^2\right)\right]\right\}. \end{aligned} \tag{52d}$$

Finally, the reduced density operator can be obtained easily from Eq. (49), being

$$\begin{aligned} \rho_1(t) = {} & \mathcal{N}_{\pm}^2 \sum_{m,n=I,II} (\pm 1)^{1-\delta_{mn}} \left\langle \beta_n^1 \middle| \beta_m^1 \right\rangle^{1-\exp(-2\mathrm{Re}\{\Lambda\}t)|W^-|^2} \\ & \times \left\langle \beta_n^2 \middle| \beta_m^2 \right\rangle^{1-\exp(-2\mathrm{Re}\{\Lambda\}t)|Z^+|^2} \mathrm{e}^{\mathrm{i}\theta_{mn}^{(3)}+\theta_{mn}^{(4)}} |\varsigma_m\rangle\langle\varsigma_n|, \end{aligned} \tag{53}$$

$$\begin{aligned} \rho_2(t) = {} & \mathcal{N}_{\pm}^2 \sum_{m,n=I,II} (\pm 1)^{1-\delta_{mn}} \left\langle \beta_n^1 \middle| \beta_m^1 \right\rangle^{1-\exp(-2\mathrm{Re}\{\Lambda\}t)|Z^-|^2} \\ & \times \left\langle \beta_n^2 \middle| \beta_m^2 \right\rangle^{1-\exp(-2\mathrm{Re}\{\Lambda\}t)|W^+|^2} \mathrm{e}^{\mathrm{i}\theta_{mn}^{(1)}+\theta_{mn}^{(2)}} |\zeta_m\rangle\langle\zeta_n|. \end{aligned} \tag{54}$$

5. State recurrence and swap dynamics

Let us suppose that the joint system $1+2$ is prepared in the superposition state

$$|\psi_{12}\rangle = \mathcal{N}_{\pm}(|\alpha\rangle \pm |-\alpha\rangle)_1 \otimes |\eta\rangle_2, \tag{55}$$

which represents a particular case of Eq. (48), where $\beta_I^1 = -\beta_{II}^1 = \alpha$ and $\beta_I^2 = \beta_{II}^2 = \eta$.

In this section we analyze, in the weak and strong coupling regimes, the effect of dissipation on two phenomena: (i) the joint-system state recurrence and (ii) the state swap between the systems. Considering the dynamics of the coupled systems, governed by the Fokker–Planck equation (37), we calculate (i) the probability that in each system the initial state recurs—the recurrence time for both systems being the same—and (ii) the probability of a swapping of states between the systems, i.e., the probability of oscillator 1 being in the initial state of oscillator 2, and vice versa. State recurrence and swap dynamics is guaranteed for bipartite coupled systems [47]. However, for a larger composite system, both dynamics depend on its topology and also on the arrangement of the coupling strengths, such that the collective eigenstates of the system have commensurate frequencies. In [35], where the present system is generalized to a network of N interacting dissipative quantum oscillators, the dependence of the recurrence and swap dynamics on the topology of the network is discussed. Here the two oscillators are coupled by a bilinear Hamiltonian which, in principle, allows state swap to occur between the systems [38].

Considering the initial superposition (55), the time-evolved joint state following from the density operator (49) reads

$$\rho_{12}(t) = \sum_{m,n=I,II} \mathcal{C}_{mn}(t)|\varsigma_m,\zeta_m\rangle\langle\varsigma_n,\zeta_n|, \tag{56}$$

where

$$\mathcal{C}_{mn}(t) = \mathcal{N}_{\pm}^2(\pm 1)^{1-\delta_{mn}} \exp\left\{-2|\alpha|^2\left[1-\left(|W^-|^2+|Z^-|^2\right)\exp\left(-2\mathrm{Re}\{\Lambda\}t\right)\right]\right\} \times \exp\left\{\mathrm{i}\left[\theta_{mn}^{(1)}+\theta_{mn}^{(3)}+\mathrm{Im}\left(\theta_{mn}^{(2)}+\theta_{mn}^{(4)}\right)\right]\right\} \tag{57}$$

and the probability of recurrence is given by

$$P_R(t) \equiv \mathrm{Tr}_{12}[\rho_{12}(t)\rho_{12}(0)] = \mathcal{N}_{\pm}^2 \sum_{m,n=I,II} \mathcal{C}_{mn}(t)\langle\varsigma_n|(|\alpha\rangle \pm |-\alpha\rangle)_1(\langle\alpha| \pm \langle-\alpha|)|\varsigma_m\rangle\langle\zeta_m|\eta\rangle_2\langle\eta|\zeta_m\rangle. \tag{58}$$

Analogously to the recurrence probability, the state-swap probability is calculated by swapping the labels of each initial state of the two fields, as defined in [38]:

$$P_S(t) \equiv \mathrm{Tr}[\rho_{12}(t)\rho_{12}(0)|_{1(2)\to 2(1)}] = \mathcal{N}_{\pm}^2 \sum_{m,n=I,II} \mathcal{C}_{mn}(t)\langle\varsigma_n|\eta\rangle_2\langle\eta|\varsigma_m\rangle\langle\zeta_m|(|\alpha\rangle \pm |-\alpha\rangle)_1(\langle\alpha| \pm \langle-\alpha|)|\zeta_m\rangle. \tag{59}$$

In Fig. 4 we plot the state-swap probability $P_S(t)$ (dotted line) and the recurrence probability $P_R(t)$ (solid line) against the scaled time λt, taking $\alpha = \eta = 1$ as real parameters. In Figs. 3A–C we set the driving field strength F to zero (so that

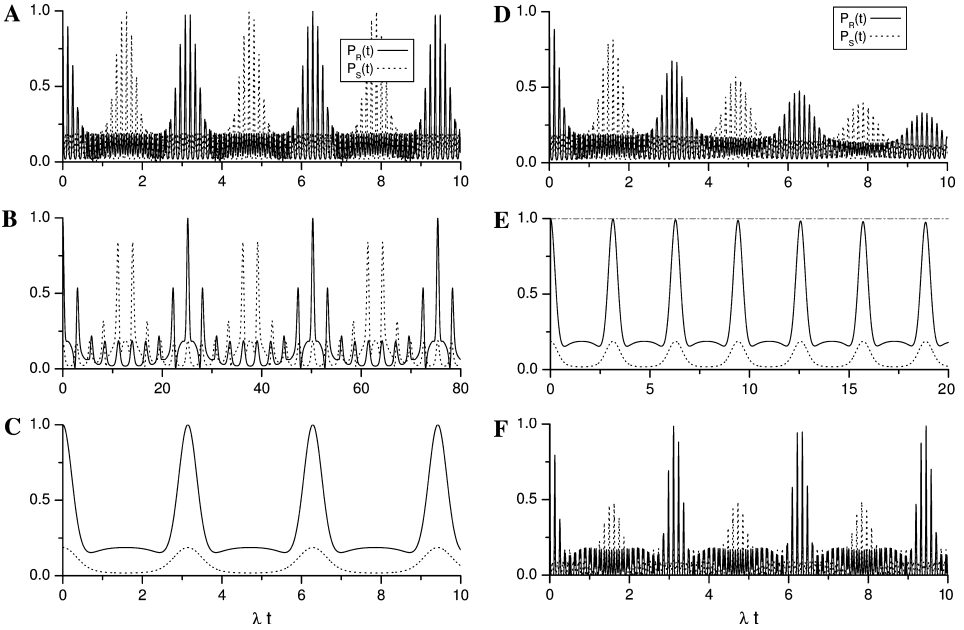

Fig. 4. State-swap probability $P_S(t)$ (dotted line) and recurrence probability $P_R(t)$ (solid line) as a function of the scaled time λt, for the factorized state $|\psi_{12}\rangle = \mathcal{N}_{\pm}(|\alpha\rangle \pm |-\alpha\rangle)_1 \otimes |\eta\rangle_2$, taking $\alpha = \eta = 1$ as real parameters. (A–C) Relaxation and driving field are disregarded and we assume (A) weak coupling, (B) an intermediate coupling, and (C) strong coupling regimes. (D and E) we set $F = 0$ but dissipation is included, considering (D) weak coupling and (E) strong coupling regimes. Finally, in (F) dissipation is disregarded and the driving field turned on.

$\omega_{10} = \omega_{20}$ and the minimum of ω_{ℓ}^{-}, occurring for $\lambda = 2\omega_{20}$, also becomes zero) and assume the absence of dissipation, so as to take these figures as references. In Fig. 4A we consider the weak coupling regime, assuming $\lambda/\omega_{10} = 2 \times 10^{-2}$ [a somewhat exaggerated ratio used to visualize better the strong oscillations of probabilities $P_R(t)$ and $P_S(t)$]. We observe (dotted line), as can be deduced from Eq. (59), that the modes will swap their states whenever

$$\lambda t_S = (2n+1)\frac{\pi}{2}, \quad n = 0, 1, 2, \ldots, \tag{60}$$

which means that in the swap time t_S, the state of mode 1 becomes $|\beta\rangle_1$, while the state of mode 2 becomes the superposition $(|\alpha\rangle \pm |-\alpha\rangle)_2$. From the solid line and Eq. (58), we observe that the joint-system state recurs whenever

$$\lambda t_R = n\pi, \quad n = 0, 1, 2, \ldots, \tag{61}$$

i.e., in the recurrence time t_R the mode 1(2) returns to its initial state $(|\alpha\rangle \pm |-\alpha\rangle)_1$ $(|\beta\rangle_2)$. It is evident that the shape of Fig. 4A results mainly from the small value of λ (compared to Ω) which defines an envelope function.

In Fig. 4B an intermediate coupling is assumed, such that $\lambda/\omega_{10} = 1$. As can be observed, the recurrence dynamics remains the same (solid line), while the swap

dynamics begins to be affected by the coupling strength. In Fig. 4C we consider the strong coupling regime where $\lambda = 2\omega_{10}$ ($\omega_{10} = \omega_{20}$), such that $\Omega/\lambda = 1$ (note that $\Omega/\lambda = \omega_{10}/\lambda + \lambda/4\omega_{20}$). As in Figs. 4A and C the recurrence process remains unchanged, still obeying Eq. (61), so that the recurrence time becomes smaller due to the strong coupling parameter λ. However, the swap dynamics is almost completely lost, the remaining oscillations arising from the non-orthogonality between the states $(|\alpha\rangle \pm |-\alpha\rangle)_1$ and $|\beta\rangle_2$.

To understand the behavior of $P_R(t)$ and $P_S(t)$ in Figs. 4B and C, we note that in the absence of dissipation the recurrence and state-swap probabilities are computed as $P_R(t) = |\langle\psi_{12}(0)|\psi_{12}(t)\rangle|^2$ and $P_S(t) = |\langle\psi_{12}(0)|\psi_{12}(t)|_{1(2)\to 2(1)}\rangle|^2$, respectively. For $P_R(t)$, the probability amplitude

$$\begin{aligned}\langle\psi_{12}(0)|\psi_{12}(t)\rangle = \mathcal{N}_{\pm}^2(&\langle\alpha|\varsigma_I\rangle\langle\eta|\zeta_I\rangle + \exp(2i\alpha G_2 \sin(\lambda t))\langle-\alpha|\varsigma_{II}\rangle\langle\eta|\zeta_{II}\rangle \\ &\pm\langle-\alpha|\varsigma_I\rangle\langle\eta|\zeta_I\rangle \pm \exp(2i\alpha G_2 \sin(\lambda t))\langle\alpha|\varsigma_{II}\rangle\langle\eta|\zeta_{II}\rangle),\end{aligned} \tag{62}$$

tends to unity under the conditions $\zeta_I, \zeta_{II} \to \eta$, $\varsigma_I \to \alpha(-\alpha)$, and $\varsigma_{II} \to -\alpha(\alpha)$, which are satisfied when $\cos \Omega t_R \cos \lambda t_R = 1$. This relation implies that

$$t_R = \frac{n\pi}{\lambda} = \frac{m\pi}{\Omega}, \tag{63}$$

where n, m are integers, both being even or odd. In Fig. 4B, the intermediate coupling $\lambda/\omega_{10} = 1$ follows from $n = (4/5)m$, such that the joint-system state recurs whenever

$$\lambda t_R = 8n\pi, \quad n = 0, 1, 2, \ldots, \tag{64}$$

a result which explains the shift in the scaled time λt observed in Fig. 4B.

Concerning the state-swap probability $P_S(t)$, we obtain the expression

$$\begin{aligned}\langle\psi_{12}(0)|_{1(2)\to 2(1)}|\psi_{12}(t)\rangle = \mathcal{N}_{\pm}^2(&\langle\alpha|\zeta_I\rangle\langle\eta|\varsigma_I\rangle + \exp(2iG_2\alpha \sin(\lambda t))\langle-\alpha|\zeta_{II}\rangle\langle\eta|\varsigma_{II}\rangle \\ &\pm\langle-\alpha|\zeta_I\rangle\langle\eta|\varsigma_I\rangle \pm \exp(2iG_2\alpha \sin(\lambda t))\langle\alpha|\zeta_{II}\rangle\langle\eta|\varsigma_{II}\rangle),\end{aligned} \tag{65}$$

which tends to unity when $\varsigma_I, \varsigma_{II} \to \eta$, $\zeta_I \to \alpha(-\alpha)$, and $\zeta_{II} \to -\alpha(\alpha)$. These conditions are satisfied only when $\sin \Omega t_S \sin \lambda\, t_S = -1$ and $G_1, G_2 \approx 0$. For the special case of $F = 0$, as in Figs. 4B and C, the condition G_1, $G_2 \approx 0$ is automatically satisfied (as can be deduced from Eqs. (43) and (44)) and the modes will swap their states whenever

$$t_S = \frac{(2n-1)\pi}{2\lambda} = \frac{(2m+1)\pi}{2\Omega}, \tag{66}$$

with the additional condition that $\sin[(n - 1/2)\pi] = -\sin[(m + 1/2)\pi]$. Therefore, the maxima of the swap probability are eliminated, as observed in Fig. 4B (for the intermediate coupling $\lambda/\omega_{10} = 1$) due to the fact that the relation $2n - 1 = 4(2m + 1)/5$ (and so $\sin \Omega t_S \sin \lambda t_S = -1$) cannot be satisfied for any pair (n,m). However, owing to the oscillations of $P_S(t)$ within the envelop function defined by $\lambda(=4\Omega/5)$, the neighborhood of these maxima still survives. Differently, in Fig. 4C (for the strong coupling regime $\Omega/\lambda = 1$), the relation $\sin \Omega t_S \sin \lambda\, t_S = \sin^2 \lambda\, t_S \neq -1$ implies that

the single maximum of the swap probability is eliminated (since $\Omega/\lambda = 1$, there are no oscillations of $P_S(t)$ but the envelope function). A heuristic explanation of the behaviors of Figs. 4B and C will be provided below. In fact, as discussed below, while the superposition state $\mathcal{N}_{\pm}(|\alpha\rangle \pm |-\alpha\rangle)_1$ swaps to oscillator 2, the coherent state $|\eta\rangle_2$ does not swap to oscillator 1, even though both return to their respective systems. Evidently, the phase mismatching between the coupling parameter λ and the field-shifted frequencies $\omega_\ell = \Omega$ (when $F = 0$), represented by the relation $\sin \Omega t_S \sin \lambda t_S = \sin^2 \lambda t_S \neq -1$, is the core of this result.

In Fig. 4D, also setting $F = 0$, we include dissipation, taking both systems with the same damping rate $\gamma_\ell^{\pm} = \Gamma/2$, where $\Gamma/\omega_{10} = 2 \times 10^{-3}$, and $\lambda/\omega_{10} = 2 \times 10^{-2}$ (as in the weak coupling regime) and observing, as expected, the relaxation of both probabilities $P_R(t)$ (solid line) and $P_S(t)$ (dotted line). To compare the relaxation of probabilities $P_R(t)$ and $P_S(t)$ in both regimes, in Fig. 4E we assume the parameters $F = 0$, $\gamma_\ell^{+} = 2\gamma_\ell^{-} = \Gamma/2$ (assuming Markovian white noise), $\Gamma/\omega_{10} = 2 \times 10^{-3}$, and $\lambda/\omega_{10} = 2$ (as in the strong coupling regime). We observe, comparing Figs. 4D and E, that in the strong coupling regime the fields recur more frequently, within the relaxation time, than in the weak coupling regime. Owing to the strong coupling, in Fig. 4E the swap dynamics is almost completely lost, as in Fig. 4C. In Fig. 4E, a dashed-dotted line has been drawn at unity to display the slow decay of $P_R(t)$.

Finally, in Fig. 4F we again disregard dissipation, but turn on the driving field, taking $F/\omega_{20} = 1$ (i.e., $\omega_{10} = 2\omega_{20}$), and $\lambda/\omega_{10} = 2 \times 10^{-2}$ (as in the weak coupling regime), and observe a reduction of the swap probability compared to the recurrence probability. (Note that the driving field occurs in the von Neumann term of Eq. (19) even though it does not influence the Liouville operator.) This behavior can be explained by the result

$$G_1 - G_2 = \frac{F}{\Omega - \lambda}, \tag{67}$$

which becomes 1/2 for the parameters considered above, preventing the swap probability from being unity, as required by the conditions $\sin \Omega t_S \sin \lambda t_S = -1$ and $G_1 - G_2 \approx 0$. We have assumed in this figure the ratio $\omega/\omega_{10} = 10^{-2}$, instead of the resonance condition $\omega/\omega_{10} = 1/2$ adopted above, to make clear the amplification effects. From Eq. (65) it follows immediately that the probability $P_S(t)$ is reduced by the factor $\exp\{-2[F/(\Omega - \lambda)]^2\}$, which explains the maximum value around 1/2 for the probability $P_S(t)$. It is worth noting that the expression (67) does not diverge for $F \neq 0$, since in the case where $\Omega = \lambda$ (and switching off the dissipation), Eq. (41) becomes

$$\frac{\partial^2 \alpha_1}{\partial t^2} - 2\Omega \frac{\partial \alpha_1}{\partial t} - \mathrm{i} F \lambda = 0, \tag{68}$$

whose solution differs from that leading to Eq. (67).

It can be argued that the state-swap and recurrence dynamics are consequences of energy transfer between modes, which in the presence of dissipation is severely reduced, as the two modes tend to reach energy equilibrium with the reservoirs and the driving field. Actually, state-swap and recurrence are properties of information

transfer rather than energy transfer between systems, even though these quantities are generally correlated. However, it can be shown [38] that for the coupling between the modes selected above, even if each mode is kept to constant energy, their states can be swapped, showing the independence of the two processes. In the presence of the relaxation process, the information transfer between modes is reduced, because of the absorption of information by the reservoirs. When the systems are strongly interacting, however, the field states recur many times on the scale of λ before the relaxation takes place. While not preventing the modes from relaxing to equilibrium with the reservoirs, the recurrence has striking consequences for short-time-scale dynamics, such as the dynamics of decoherence discussed below.

6. Coherence properties

So far we have analyzed the dynamics of strongly interacting modes 1 and 2 to discuss the recurrence and state-swap processes. Now we analyze, also in the strong coupling regime, with the driving field switched off ($F = 0$) and the reservoirs at absolute zero ($T = 0$), the decoherence dynamics of the joint state described by the density operator ρ_{12}, and of the state of system 1 (2), described by $\rho_1 = \mathrm{Tr}_2\rho_{12}$ ($\rho_2 = \mathrm{Tr}_1\rho_{12}$). In this section, we also consider the case of identical dissipative systems, $\gamma_\ell^\pm = \gamma^\pm$. The case of different decay rates will be analyzed subsequently. We consider three different initial joint states: first, the disentangled state, given by Eq. (55), and then the entanglements which are eigenstates associated with the normal modes $\omega_\ell^\pm$, derived from Eq. (48): with $\beta_I^1 = \beta_{II}^2 = \alpha$ and $\beta_I^2 = \beta_{II}^1 = -\alpha$ we obtain the eigenstate

$$\left|\varphi_{12}^-\right\rangle = \mathcal{N}_\pm(|\alpha, -\alpha\rangle_{12} \pm |-\alpha, \alpha\rangle_{12}), \tag{69}$$

associated with the normal mode ω_ℓ^-, and with $\beta_I^1 = \beta_I^2 = \alpha$ and $\beta_{II}^2 = \beta_{II}^1 = -\alpha$, we obtain

$$\left|\varphi_{12}^+\right\rangle = \mathcal{N}_\pm(|\alpha, \alpha\rangle_{12} \pm |-\alpha, -\alpha\rangle_{12}), \tag{70}$$

which is the eigenstate associated with ω_ℓ^+.

6.1. Decoherence time of the state $|\psi_{12}\rangle = \mathcal{N}_\pm(|\alpha\rangle \pm |-\alpha\rangle)_1 \otimes |\eta\rangle_2$

The coherence of the joint state (55) is given, essentially, by the term

$$\exp\{-2|\alpha|^2[1 - (|W^-|^2 + |Z^-|^2)\exp(-2\mathrm{Re}\{\Lambda\}t)]\}, \tag{71}$$

coming from the off-diagonal coefficients of the density operator in Eq. (56). In the strong coupling regime, the exponential decay in Eq. (71), computed from Eqs. (42a), (42b), reduces to the form

$$\exp[-|\alpha|^2(2 - \mathrm{e}^{-(\gamma_1^+ + \gamma_2^+)t} - \mathrm{e}^{-(\gamma_1^- + \gamma_2^-)t})]. \tag{72}$$

Assuming identical dissipative systems, $\gamma_\ell^\pm = \gamma^\pm$, Eq. (72) simplifies to

$$\exp[-|\alpha|^2(2-\mathrm{e}^{-2\gamma^+ t}-\mathrm{e}^{-2\gamma^- t})], \tag{73}$$

resulting in a decoherence time for the joint system given by

$$\tau_D = [2|\alpha|^2(\gamma^+ + \gamma^-)]^{-1}. \tag{74}$$

This decoherence time has to be compared with that for an isolated mode in the superposition state $\mathcal{N}_\pm(|\alpha\rangle \pm |-\alpha\rangle)$ (also obtained from the weak coupling regime: $\gamma^\pm = \Gamma/2$), following from the exponential decay

$$\exp[-2|\alpha|^2(1-\mathrm{e}^{-\Gamma t})] \tag{75}$$

and given by the well-known expression $\tau_D \approx \tau_R/2|\alpha|^2 \equiv \mathcal{T}_D$, where $\tau_R = \Gamma^{-1}$ stands for the relaxation time of the system. Analyzing the decoherence process in the light of the spectral densities considered in Section 3, we observe that for Markovian white noise (M), where $\gamma^- = \gamma^+/2 = \Gamma/4$, the decoherence time in Eq. (74) rises to

$$\tau_D^M \approx 4\mathcal{T}_D/3. \tag{76}$$

For the Lorentzian spectral density (L), where $\gamma^\pm = \varepsilon^\pm\Gamma/2 \ll \Gamma$, we obtain the result

$$\tau_D^L \approx 2\mathcal{T}_D/(\varepsilon^+ + \varepsilon^-), \tag{77}$$

which becomes large as the reservoir spectral density decreases around the effective frequency $\omega_\ell^\pm = \omega^\pm$. We stress that for the case where $\varepsilon^+ = \varepsilon^-$ (i.e., $\gamma^+ = \gamma^-$) the cross-decay channel is null.

Finally, for a wide Lorentzian spectral density (WL), where $\gamma^- = \varepsilon^-\Gamma/2 \ll \Gamma$ and $\gamma^+ = \Gamma/2$, we obtain from Eq. (74), the value

$$\tau_D^{WL} \approx 2\mathcal{T}_D. \tag{78}$$

Therefore, for a wide Lorentzian spectral density we obtain a decoherence time for strongly coupled systems which is twice as long as in the weak-coupling regime. The mechanism behind these improved decoherence times is that in the strong coupling regime (where the natural frequency $\omega_{\ell 0}$ of the systems splits into two effective frequencies $\omega_\ell^\pm = \omega_\ell \pm \lambda$) the spectral density of the reservoir plays a decisive role in the damping rate, which also splits into two Lorentzian functions. When the oscillator effective frequency $\omega_\ell^\pm$ shifts to regions where the spectral density of the reservoir is significantly smaller than that around $\omega_{\ell 0}$, the damping rate becomes smaller than its value in the weak coupling regime. Despite the spectral densities, the competition between the cross-decay and the usual channels is the reason for the computed delay of the decoherence process.

Still regarding state (55) and the strong coupling regime, focusing on the reduced systems, we obtain from Eqs. (53) and (54) the density operators

$$\rho_1(t) = \mathcal{N}_\pm^2 \sum_{m,n=I,II} (\pm 1)^{1-\delta_{mn}} \left\langle \beta_n^1 \middle| \beta_m^1 \right\rangle^{1-\mathcal{F}(\lambda t)/4} \mathrm{e}^{\mathrm{i}\theta_{mn}^{(3)} + \mathrm{i}\mathrm{Im}\theta_{mn}^{(4)}} |\zeta_m\rangle\langle\zeta_n|, \tag{79}$$

$$\rho_2(t) = \mathcal{N}_\pm^2 \sum_{m,n=I,II} (\pm 1)^{1-\delta_{mn}} \left\langle \beta_n^1 \middle| \beta_m^1 \right\rangle^{1-\mathcal{F}(\lambda t+\pi/2)/4} \mathrm{e}^{\mathrm{i}\theta_{mn}^{(1)} + \mathrm{i}\mathrm{Im}\theta_{mn}^{(2)}} |\zeta_m\rangle\langle\zeta_n|, \tag{80}$$

where

$$\mathcal{F}(\lambda t) = \exp\left[-(\gamma_1^+ + \gamma_2^+)t\right] + \exp\left[-(\gamma_1^- + \gamma_2^-)t\right] + 2\cos(2\lambda t) \times \exp\left[-(\gamma_1^+ + \gamma_2^+ + \gamma_1^- + \gamma_2^-)t/2\right]. \tag{81}$$

Observe that for identical systems, $\gamma_\ell^\pm = \gamma^\pm$, the decoherence of the reduced state in oscillator 1 is given by

$$\exp\{-2|\alpha|^2[1 - \tfrac{1}{4}(e^{-2\gamma^+ t} + e^{-2\gamma^- t} + 2\cos(2\lambda t)e^{-(\gamma^+ + \gamma^-)t})]\} \tag{82}$$

while for the state in oscillator 2 it is

$$\exp\{-2|\alpha|^2[1 - \tfrac{1}{4}(e^{-2\gamma^+ t} + e^{-2\gamma^- t} + 2\cos(2\lambda t + \pi)e^{-(\gamma^+ + \gamma^-)t})]\}. \tag{83}$$

It is easily shown that the expressions in Eqs. (82) and (83), associated with the decoherence times of the states of systems 1 and 2, respectively, oscillate below the curve for the coherence decay of the joint system given by expression (73). In Fig. 5, assuming Markovian white noise and setting the fictitious ratio $\lambda/\Gamma = 5$ to make the oscillations clear, the dashed and dotted lines refer to the decoherence dynamics of systems 1 and 2, dictated by Eqs. (82) and (83), respectively. The solid line represents the coherence decay derived from Eq. (73) and the dashed-dotted line indicates the coherence decay for an isolated mode, computed from Eq. (75). Therefore, for the special case of the initially disentangled state given by Eq. (55), the decoherence times of systems 1 and 2 coincide with that of the joint system.

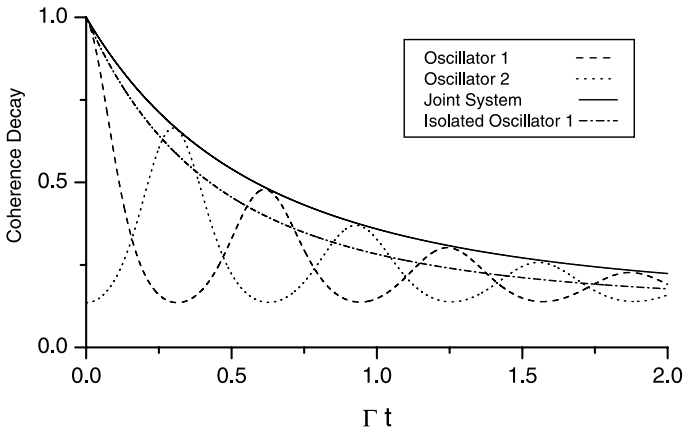

Fig. 5. Decoherence dynamics for the factorized state $|\psi_{12}\rangle = \mathcal{N}_\pm(|\alpha\rangle \pm |-\alpha\rangle)_1 \otimes |\eta\rangle_2$, assuming both oscillators with the same damping factor. Coherence decays of oscillator 1 (dashed line), oscillator 2 (dotted line), joint system (solid line), and an isolated oscillator with damping rate Γ_1 (dashed-dotted line) are indicated.

6.2. Decoherence time of the state $|\varphi_{12}^{-}\rangle = \mathcal{N}_{\pm}(|\alpha,-\alpha\rangle_{12} \pm |-\alpha,\alpha\rangle_{12})$

Next, we analyze the decoherence dynamics of the entangled state (69) for the joint system. The decoherence process of this joint state, in the strong coupling regime, is given by the exponential decay

$$\exp[-4|\alpha|^2(1-\mathrm{e}^{-(\gamma_1^- + \gamma_2^-)t})], \tag{84}$$

which takes into account only the decay rate of the system–reservoir coupling around the effective frequency ω_ℓ^-. At this point it is interesting to identify the contribution of the cross-decay channel to the decoherence process, rewriting Eq. (84) as

$$\exp\left\{-4|\alpha|^2\left(1-\exp\left[-\sum_\ell(\gamma_\ell^+ + \gamma_\ell^-)t/2\right]\exp\left[\sum_\ell(\gamma_\ell^+ - \gamma_\ell^-)t/2\right]\right)\right\}. \tag{85}$$

In this expression, the term $\exp[\sum_\ell(\gamma_\ell^+ - \gamma_\ell^-)t/2]$ comes from the cross-decay channel and it is evident that for $\sum_\ell(\gamma_\ell^+ - \gamma_\ell^-) > 0$, its contribution makes the exponential decay slower. Assuming identical dissipative systems, $\gamma_\ell^- = \gamma^-$, the expression (84) simplifies to

$$\exp[-4|\alpha|^2(1-\mathrm{e}^{-2\gamma^- t})], \tag{86}$$

leading to the decoherence time $(8|\alpha|^2\gamma^-)^{-1}$, which is $\mathcal{T}_D/2$ in the weak coupling regime, as expected. However, in the strong coupling regime, this decoherence time for an entangled state is equal to $\mathcal{T}_D$ for Markovian white noise and is significantly improved for both Lorentzian spectral densities, where we obtain $\mathcal{T}_D/2\varepsilon^-$.

6.3. Decoherence time of the state $|\varphi_{12}^{+}\rangle = \mathcal{N}_{\pm}(|\alpha,\alpha\rangle_{12} \pm |-\alpha,-\alpha\rangle_{12})$

The decoherence process of the joint state $|\varphi_{12}^{+}\rangle$, in the strong coupling regime, is given by the exponential decay

$$\exp[-4|\alpha|^2(1-\mathrm{e}^{-(\gamma_1^+ + \gamma_2^+)t})], \tag{87}$$

depending only on the decay rate of the system–reservoir coupling around the effective frequency ω_ℓ^+. Rewriting Eq. (87) as

$$\exp\left\{-4|\alpha|^2\left(1-\exp\left[-\sum_\ell(\gamma_\ell^+ + \gamma_\ell^-)t/2\right]\exp\left[-\sum_\ell(\gamma_\ell^+ - \gamma_\ell^-)t/2\right]\right)\right\}, \tag{88}$$

we identify the term $\exp[-\sum_\ell(\gamma_\ell^+ - \gamma_\ell^-)t/2]$ as coming from the cross-decay channel. It is evident that for $\sum_\ell(\gamma_\ell^+ - \gamma_\ell^-) > 0$, its contribution speeds up the exponential decay, in contrast to the above situation where the eigenstate of the normal mode ω_ℓ^- is considered. For $\gamma_\ell^+ = \gamma^+$, Eq. (87) simplifies to

$$\exp[-4|\alpha|^2(1-\mathrm{e}^{-2\gamma^+ t})], \tag{89}$$

and the decoherence time $(8|\alpha|^2\gamma^+)^{-1}$ becomes $\mathcal{T}_D/2$ for the weak coupling regime and also for both spectral densities, Markovian white noise and the wide Lorentzian spectral noise, in the strong coupling regime. For the Lorentzian spectral density, we

obtain $\mathcal{T}_D/2\varepsilon^+$. In the light of the above results we conclude, apart from the dependence of the decoherence time upon the reservoir spectral densities, that the eigenstate associated with the normal mode ω_ℓ^- is less susceptible to decoherence than that associated with ω_ℓ^+.

7. Improving the quality factor of a dissipative system

Let us now turn to a central result, which is the effect of the coupling λ on the decoherence process for states of oscillators with different damping rates Γ_1 and Γ_2. We assume that the state of the whole system is given by Eq. (55) and that oscillator 2 has a better quality factor than oscillator 1 (i.e., $\Gamma_1 = \Gamma \gg \Gamma_2$), where we have the superposition $\mathcal{N}_\pm(|\alpha\rangle \pm |-\alpha\rangle)_1$ which we want to protect. The decoherence of state 1, following from Eq. (79), is then governed by the exponential decay

$$\exp\left\{-2|\alpha|^2\left[1-\frac{1}{4}\left(\mathrm{e}^{-\gamma^- t}+\mathrm{e}^{-\gamma^+ t}+2\cos(2\lambda t)\,\mathrm{e}^{-(\gamma^+ +\gamma^-)t/2}\right)\right]\right\} \tag{90}$$

while for the field state 2, following from (80), it is governed by

$$\exp\left\{-2|\alpha|^2\left[1-\frac{1}{4}\left(\mathrm{e}^{-\gamma^- t}+\mathrm{e}^{-\gamma^+ t}+2\cos(2\lambda t+\pi)\mathrm{e}^{-(\gamma^+ +\gamma^-)t/2}\right)\right]\right\}. \tag{91}$$

These expressions are to be compared with Eqs. (82) and (83), respectively, where we have assumed the same quality factors for both oscillators. The decoherence times obtained from Eqs. (90) and (91) have an upper limit given by the exponential decay for the joint system

$$\exp[-|\alpha|^2(2-\mathrm{e}^{-\gamma^+ t}-\mathrm{e}^{-\gamma^- t})], \tag{92}$$

which is derived from Eq. (72). This exponential decay leads to a decoherence time given by

$$\tau_D \approx [|\alpha|^2(\gamma^+ + \gamma^-)]^{-1}, \tag{93}$$

which is twice the result found in Eq. (74), for the case of identical dissipative systems ($\gamma_\ell^\pm = \gamma^\pm$), whatever the spectral density of the reservoir. Therefore, even in the weak coupling regime, the decoherence time of a system is improved when it is coupled to another system with a better quality factor. We stress that this conclusion holds only when $\lambda \gg \gamma_\ell^\pm$, a situation we have assumed even for the weak coupling regime. Evidently, when $\lambda \lessapprox \gamma_\ell^\pm$, so that the recurrence-swap dynamics does not take place effectively before the relaxation time, the quality factor of a system cannot be improved by coupling it to another system of better quality.

In Fig. 6, assuming the weak coupling regime, $\gamma_\ell^\pm = \Gamma_\ell/2$, with $\Gamma_1/\Gamma_2 = 10^2$ and $\lambda/\Gamma_1 = 5$ (a ratio chosen to show the dissipative dynamics clearly), the dashed and dotted lines refer to the decoherence dynamics of systems 1 and 2, derived from Eqs. (90) and (91), respectively. The solid line represents the coherence decay for the joint system derived from Eq. (92) and the dashed-dotted line indicates the coherence decay for the isolated mode 1, where the superposition state $\mathcal{N}_\pm(|\alpha\rangle \pm |-\alpha\rangle)_1$ is

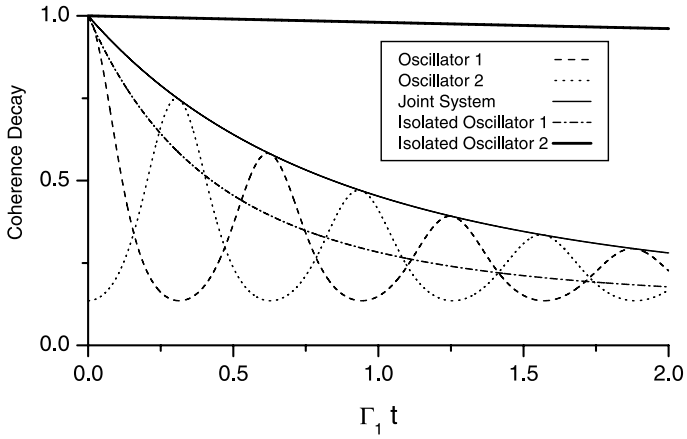

Fig. 6. Decoherence dynamics for the factorized state $|\psi_{12}\rangle = \mathcal{N}_{\pm}(|\alpha\rangle \pm |-\alpha\rangle)_1 \otimes |\eta\rangle_2$, assuming that the damping rate of oscillator 1 is larger than that of oscillator 2. The dashed (dotted) line refers to the decoherence dynamics of oscillator 1(2), while the solid (dashed-dotted) line represents the coherence decay of the joint system (an isolated system with the damping rate of oscillator 1), respectively. The thick solid line represents the coherence decay of a superposition state $\mathcal{N}_{\pm}(|\alpha\rangle \pm |-\alpha\rangle)_2$ prepared in an isolated oscillator 2.

prepared, computed from Eq. (75). However, while the bad-quality system 1 gets better when coupled to a good-quality system 2, the latter, in turn, gets worse. In fact, the thick solid line in Fig. 6, representing the decoherence process of the superposition $\mathcal{N}_{\pm}(|\alpha\rangle \pm |-\alpha\rangle)_2$ prepared in an isolated good-quality system 2, displays a slower decay rate than the solid line when system 2 is coupled to a bad-quality system 1. In conclusion, in a network made of two oscillators with different quality factors, the good-quality oscillator gets worse, while the bad-quality oscillator gets better. We hope that this process may be even improved by extending the coupling of a bad-quality oscillator to a higher number of good-quality oscillators.

Finally, we note that the above result can be theoretically employed to protect quantum superposition states generated, via atom–field interaction, in open cavities. By coupling an open bad-quality cavity, where we have prepared a quantum superposition, to a closed good-quality cavity, we can protect the superposition through the coupling between the cavities and, further, in an appropriate recurrence time, we can recover that superposition state in the open cavity. The process works as if the original superposition coherence is protected from the dissipative mechanism by the recurrence-swap dynamics, much like a system which is put in contact with a high-temperature reservoir, but is intermittently brought into contact with a low-temperature reservoir. If the interval between contacts is fast enough, the system will take longer to relax to the hot reservoir temperature than it would in the absence of the cold reservoir. Of course, this analogy has to be considered cautiously, since temperature and coherence are very different features.

In the next section, we discuss how the original superposition state can be recovered in the bad-quality system after its coupling with the good-quality system.

8. Entropy excess

To clarify the role the state-swap processes play in the coherence dynamics, we consider the superposition state in Eq. (55), $|\psi_{12}\rangle = \mathcal{N}_{\pm}(|\alpha\rangle \pm |-\alpha\rangle)_1 \otimes |\eta\rangle_2$, and plot, in Figs. 7A and B, the probabilities

$$\mathcal{P}_\ell(t) = \langle\psi_m|\rho_\ell(t)|\psi_m\rangle, \tag{94}$$

of finding the superposition state $|\psi_1\rangle = \mathcal{N}_{\pm}(|\alpha\rangle \pm |-\alpha\rangle)_1$ and the coherent state $|\psi_2\rangle = |\eta\rangle_2$ in oscillator ℓ. In these figures we assume the strong coupling regime ($\lambda/\omega_{10} = 2$), identical dissipative systems ($\gamma_\ell^{\pm} = \gamma^{\pm}$), and Markovian white noise ($\gamma^{+} = 2\gamma^{-} = \Gamma/2$). The ratio $\lambda/\Gamma = 20$ is set to a fictitious scale to make clear the state-swap and state-recurrence dynamics, as the strong oscillations obtained with a realistic λ would be blurred by the slow (dissipative) dynamics.

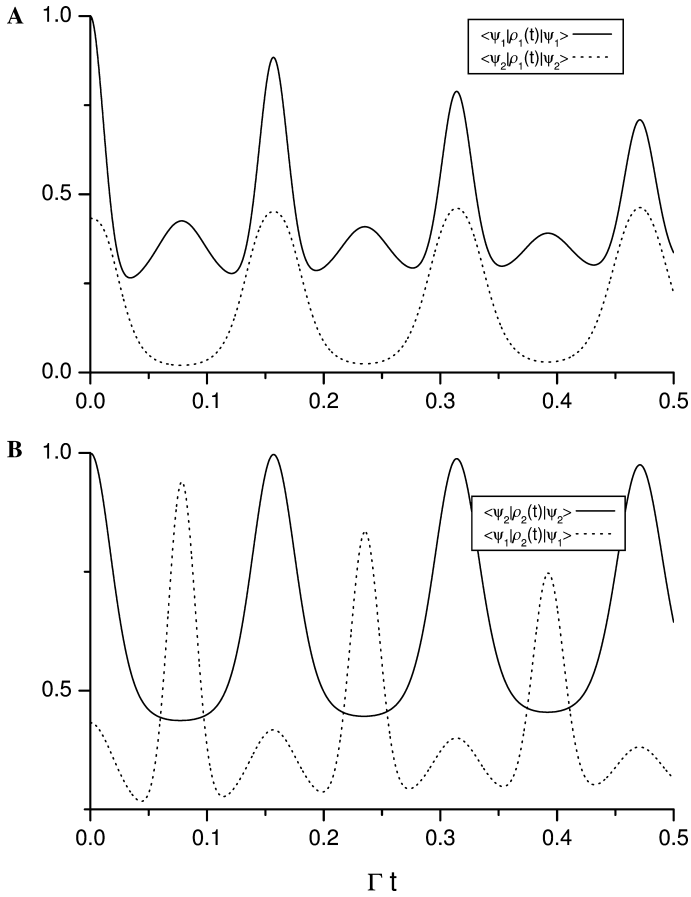

Fig. 7. Probability $\mathcal{P}_\ell(t) = \langle\psi_m|\rho_\ell(t)|\psi_m\rangle$, of finding the superposition state $|\psi_1\rangle = \mathcal{N}_{\pm}(|\alpha\rangle \pm |-\alpha\rangle)_1$ and the coherent state $|\psi_2\rangle = |\eta\rangle_2$ in oscillator ℓ. We consider (A) $\ell = 1$ and (B) $\ell = 2$. In these figures the strong coupling regime is assumed together with identical dissipative systems and Markovian white noise.

From the solid line in Fig. 7A, we observe that the superposition $|\psi_1\rangle$ recurs to oscillator 1, despite the dissipative process. However, the coherent state $|\eta\rangle_2$ does not swap to oscillator 1, as indicated by the dotted line. In fact, the swapping of the coherent state $|\eta\rangle_2$ to oscillator 1 would be indicated by the occurrence of maxima of the dotted line between those of the solid line. In Fig. 7B we observe that the coherent state $|\eta\rangle_2$ recurs to oscillator 2, as indicated by the solid line. Moreover, the state $|\psi_1\rangle$ also swaps to oscillator 2 (dotted line), indicating that the superposition $\mathcal{N}_{\pm}(|\alpha\rangle \pm |-\alpha\rangle)$ is completely interchanged between the systems, differently from the coherent state which does not swap to oscillator 1.

Therefore, from Fig. 7A we conclude that the superposition state $\mathcal{N}_{\pm}(|\alpha\rangle \pm |-\alpha\rangle)$ prepared in a bad-quality system and protected from decoherence by coupling this system to a good-quality one, can easily be recovered in system 1 by switching off the coupling at the recurrence time $t_R = n\pi/\lambda$, $n = 0, 1, 2, \ldots$ After this time, the superposition state will be in oscillator 1 with a fidelity less than unity due to the dissipative process.

In Figs. 8A and B we plot the linear entropy for the joint state in Eq. (55) ($\mathcal{S}_{12} = 1 - \mathrm{Tr}\rho_{12}^2$) and the reduced states of oscillators 1 and 2 ($\mathcal{S}_\ell = 1 - \mathrm{Tr}\rho_\ell^2$). In these figures we employ the same paramet–ers considered in Fig. 7, except that in Fig. 8B we use the ratio $\lambda/\Gamma = 2$, instead of $\lambda/\Gamma = 20$, to show clearly the dissipative dynamics. In Fig. 8A we analyze the recurrence-swap dynamics until around the correlation time τ_C, defined as the time when the entropy $\mathcal{S}_1(\mathcal{S}_2)$ goes to about 0.01 at the swap (recurrence) time. In fact, as shown in Fig. 8A, the minima of the entropy $\mathcal{S}_\ell$ move away from zero due to the development of an inevitable correlation between the oscillators (due to the cross-decay channel) which thus become permanently entangled. This correlation time, estimated as the time when the minima of $\mathcal{S}_\ell$ approach 0.01, is given by

$$\tau_C \approx \frac{1}{5|\alpha|\sum_\ell(\gamma_\ell^+ - \gamma_\ell^-)}. \tag{95}$$

From Eq. (95) we conclude that for the weak coupling regime, where $\gamma_\ell^+ = \gamma_\ell^-$, the correlation time goes to infinity, i.e., the entropy $\mathcal{S}_1(\mathcal{S}_2)$ always returns to zero in the swap (recurrence) time. Therefore, in the weak coupling regime the oscillators do not get permanently entangled (due to the absence of the cross-decay channel) and, since $\mathcal{S}_1(\mathcal{S}_2)$ always returns to zero in the swap (recurrence) time, one is always able to recover a superposition state of a bad-quality oscillator coupled to a good-quality one. However, even in the strong coupling regime the correlation developed between the oscillators could not affect the process of recovering a superposition state of a bad-quality oscillator coupled to a good-quality one. Since the ratio τ_C/τ_D obeys

$$\frac{\tau_C}{\tau_D} \approx \frac{|\alpha|}{5}\frac{\sum_\ell(\gamma_\ell^+ + \gamma_\ell^-)}{\sum_\ell(\gamma_\ell^+ - \gamma_\ell^-)}, \tag{96}$$

for $\tau_C/\tau_D \gtrsim 1$ one can always recover the superposition state $\mathcal{N}_{\pm}(|\alpha\rangle \pm |-\alpha\rangle)$, with a considerable fidelity, in spite of the process of entanglement between the oscillators.

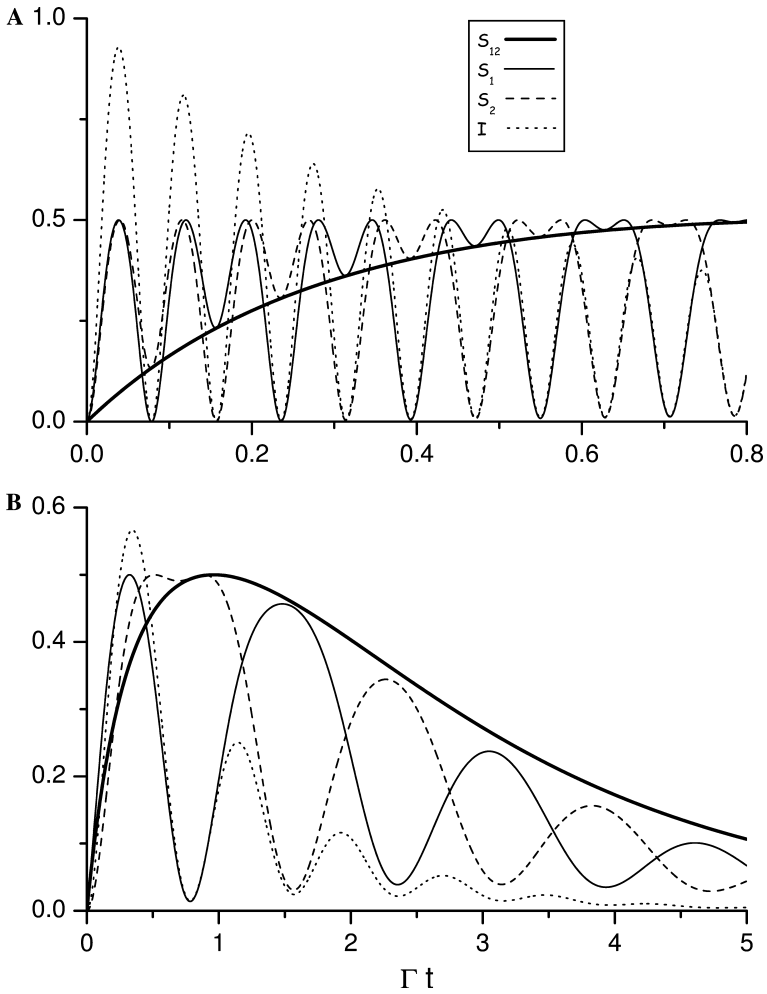

Fig. 8. Linear entropy for the joint state ($\mathcal{S}_{12} = 1 - \mathrm{Tr}\rho_{12}$), represented by the thick solid line, and the reduced states of oscillators 1 and 2 ($\mathcal{S}_\ell = 1 - \mathrm{Tr}\rho_\ell$), represented by solid and dashed lines, respectively. The dotted line indicates the excess entropy. (A) The recurrence-swap dynamics is plotted until around the correlation time τ_C when a permanent correlation is developed between the oscillators. (B) We are concerned with the relaxation of the network.

The overall picture coming from Fig. 8A is that the recurrence dynamics due to the strong coupling between the oscillators tends to restore the coherence of the initial states while the dissipative dynamics promotes the decoherence process. In Fig. 8B the linear entropy of the joint state $\mathcal{S}_{12}$, represented by the thick solid line, starts from zero, goes to a maximum due to the decoherence process and then returns to zero, since in the asymptotic limit both oscillators reach a pure state: the vacuum or some coherent state whose excitation depends on the amplification parameter F. Meanwhile, as shown in Fig. 8A, the linear entropy $\mathcal{S}_\ell$ of the reduced state of

oscillator ℓ, oscillates between zero and 0.5. The linear entropy $\mathcal{S}_1(\mathcal{S}_2)$, solid (dashed) line, becomes zero when oscillator 1(2) assumes the state $|-\eta\rangle_1(|\eta\rangle_2)$, as can be computed from Eqs. (51a) and (51b). At the same time, $\mathcal{S}_2(\mathcal{S}_1)$ bump into the thick solid line representing the linear entropy for the joint state of the system $\mathcal{S}_{12}$, from above, indicating that the superposition $|\psi_1\rangle$ has swapped (recurred) to oscillator 2(1) on its way to decoherence. The maximal correlation between fields occurs at the points where the recurrence and swap curves cross, as illustrated by the dotted line representing the excess entropy, defined as

$$\mathcal{I} \equiv \mathcal{S}_1 + \mathcal{S}_2 - \mathcal{S}_{12}. \tag{97}$$

We also observe from the dotted line that the minima of the excess entropy $\mathcal{I}$ move away from zero, due to the development of an inevitable correlation between the oscillators. Returning to Fig. 8B, after reaching its maximum the correlation $\mathcal{S}_{12}$ decays exponentially as a result of the dissipation and the driving field, attaining zero in the asymptotic limit when there is no correlation between the fields described by stationary factorized coherent states. During the decay of correlation $\mathcal{S}_{12}$, the linear entropy $\mathcal{S}_\ell$ of the reduced state of oscillator ℓ does not attain the value $\mathcal{S}_{12}$, due to the correlation described by the excess entropy $\mathcal{I}$.

9. Conclusion

We have presented a comprehensive treatment of the coherence dynamics in a network composed of two coupled dissipative oscillators. First, we have derived a master equation for both regimes of weak and strong coupling between the oscillators. In the weak coupling regime the dissipative mechanism of the individual oscillators is not significantly affected by their interaction, which appears only in the von Neumann term of the master equation. However, in the strong coupling regime the time evolution of the density operator of the joint system is modified by a cross-decay channel represented by a Liouville operator $\mathcal{L}_{12}\rho_{12}$ accounting for the coupling between the oscillators. The appearance of this cross-decay channel leads to interesting properties of the coherence dynamics of strongly coupled oscillators.

After the mathematical development, we first analyzed the state-swap and the state-recurrence dynamics, i.e., the probability that each oscillator returns to its initial state and the probability of state swapping between the oscillators, respectively. In particular, we have analyzed these processes for the case where both oscillators, prepared in the joint state $\mathcal{N}_\pm(|\alpha\rangle \pm |-\alpha\rangle)_1 \otimes |\eta\rangle_2$, present the same quality factor Γ. In the weak coupling regime the recurrence and swap processes are fully accomplished apart from the relaxation of the field states due to dissipation. On the way to the strong coupling regime the recurrence process remains unchanged while the swap dynamics is gradually lost as the coupling gets stronger. In the strong coupling regime the swap dynamics is lost due to phase mismatching between the coupling parameter λ and the field-shifted frequencies ω_ℓ, as explained in Section 5. Evidently, in the strong coupling regime the field states recur much more often than in the weak coupling regime before the relaxation takes place.

Next, aware of the decoherence dynamics in the weak coupling regime, governed by the usual master equation (21) where a Liouville operator $\mathcal{L}_\ell \rho_{12}$ accounts for the effect of the reservoir on oscillator ℓ, we turn to the decoherence process in the strong coupling regime. In this regime, the normal-mode frequencies ($\omega_\ell^\pm = \omega_\ell \pm \lambda$) of the coupled systems are strongly shifted, away from the oscillator frequencies $\omega_{\ell 0}$, to regions of the reservoir frequency spaces where the spectral densities may be significantly different from that around $\omega_{\ell 0}$. As the spectral densities of the reservoirs play an important role in this regime, three different spectral functions were considered for our analysis of the decoherence process. When the normal-mode frequency ω_ℓ^- is shifted to regions around the origin of the frequency space, even for Markovian white noise the coupling parameter of oscillator ℓ with its reservoir, around ω_ℓ^-, becomes half its value around ω_ℓ^+ (i.e., $\gamma_\ell^- = \Gamma/4$). When considering, instead, a Lorentzian spectral function, which approaches zero around the origin of the reservoir frequency space, the coupling constant γ_ℓ^- becomes even smaller, resulting in decoherence times for the joint and the reduced system states significantly longer than the result computed for a single system plus reservoir. In Section 6 the decoherence times for three different states of the composed system are computed, considering the three distinct reservoir spectral functions. Apart from the dependence of the decoherence time upon the reservoir spectral density, we stress that the coherence decay of the eigenstate of the normal mode ω_ℓ^- becomes slower than that for the eigenstate of the normal mode ω_ℓ^+.

As discussed in Section 3, apart from the possibility of considering particular physical systems with appropriate reservoir spectral densities, it is possible that specific spectral functions could be achieved through engineered reservoirs. The difficult task of engineering strong interactions between the oscillators, together with the achievement of specific reservoir spectral functions, are the most sensitive problems in the way of the physical implementation of the network here proposed. However, this proposal might provide a motivation for future theoretical and experimental investigations. In particular, the proposal could be applied to test the Markovian white noise approximation or to probe the reservoir spectral functions.

When considering the two systems to have different damping rates Γ_1 and Γ_2 (with $\lambda \gg \Gamma_1, \Gamma_2$) we demonstrated that the coupling between the systems, independently of its strength, makes the good-quality system worse and the bad-quality system better. This result can be employed to improve the quality factor of a cavity, and thus to protect quantum superposition states generated, via atom–field interaction, in open bad-quality cavities coupled to closed good-quality ones. Evidently, this results holds for the weak coupling regime because we have assumed that the coupling strength λ is significantly larger than the system damping rates even for that regime. In fact, when considering $\lambda \gg \Gamma_\ell$, the computed improvement of the quality factor of a system follows from the recurrence-swap dynamics which take place many times before the relaxation time, protecting in a good-quality system a field state originally prepared in a bad-quality one.

Finally, we have developed a careful analysis of the entropy excess in our network. Supposing that the joint system is prepared in the factorized state $|\psi_{12}\rangle = \mathcal{N}_\pm(|\alpha\rangle \pm |-\alpha\rangle)_1 \otimes |\eta\rangle_2$, we observed that in the weak-coupling regime the

recurrence-swap dynamics take place uninterruptedly until the relaxation process rules it out, i.e., the entropy excess always returns to zero in the recurrence and swap times. Therefore, in the weak-coupling regime both oscillators always get disentangled in the recurrence and swap times. Differently, in the strong coupling regime a correlation is developed between the states $\mathcal{N}_{\pm}(|\alpha\rangle \pm |-\alpha\rangle)$ and $|\eta\rangle$, in a such way that they get permanently entangled after a time interval we have called the correlation time. In this way, one cannot recuperate—with a fidelity equal to unity—a superposition state $\mathcal{N}_{\pm}(|\alpha\rangle \pm |-\alpha\rangle)$ prepared in a bad-quality system and protected from decoherence through a strong coupling of such system with a good-quality one. However, we computed the amplitude $|\alpha|$ where the correlation time becomes longer than the decoherence time, allowing the recuperation of the superposition state $\mathcal{N}_{\pm}(|\alpha\rangle \pm |-\alpha\rangle)$ with a good fidelity.

One of the main restrictions argued against quantum computation is that even if each individual logic unit were only slightly affected by the decoherence process, the coupling of a large number of such logic cells, for an actual implementation such as the factorization of large numbers [14,48], would decrease the decoherence time in such a way that the whole computing process would be seriously compromised [16]. Here we have shown, at least for two strongly coupled sites, that the decoherence process is not dictated simply by the excitation of the state involved in the logic operation and the damping decay rate of the logic cells. In a strongly interacting quantum network the decoherence process is delayed by the cross-decay channel arising from the strong coupling between the logic cells. In fact it may occur that for many coupled sites, as for the two coupled cavities presented in this paper, the decoherence time increases. We again refer to the monogamy of entanglement discussed in [36]. Therefore, the discussion about strongly interacting oscillators we have presented here is central to understand the decoherence process in a quantum network; specifically, our conclusion is that the decoherence time depends not only on the excitation of the entanglement involved in the logic operation but also on the coupling strength between the logic units.

Acknowledgments

We wish to express thanks for the support from FAPESP (under contracts #99/11859-3, #00/15084-5, and #02/02633-6) and CNPq (Intituto do Milênio de Informação Quântica), Brazilian agencies. We also thank R.M. Serra, C.J. Villas-Bôas, V.V. Dodonov, and A.F.R. de Toledo Piza for helpful discussions.

References

[1] J. von Neumann, *Mathematical Foundations of Quantum Mechanics*, Translated by R.T. Beyer, Princeton University Press (1955).
[2] W.H. Zurek, Phys. Rev. D 24 (1981) 1516;
Phys. Rev. D 26 (1982) 1862;
Phys. Today 44 (10) (1991) 36.

[3] A.O. Caldeira, A.J. Leggett, Ann. Phys. 149 (1983) 374;
A.O. Caldeira, A.J. Laggett, Phys. A 121 (1983) 587.
[4] M. Brune, E. Hagley, J. Dreyer, X. Maitre, A. Maali, C. Wunderlich, J.M. Raimond, S. Haroche, Phys. Rev. Lett. 77 (1996) 4887.
[5] D.M. Meekhof, C. Monroe, B.E. King, W.M. Itano, D.J. Wineland, Phys. Rev. Lett. 76 (1996) 1796.
[6] B.R. Mollow, R.J. Glauber, Phys. Rev. 160 (1967) 1076;
B.R. Mollow, R.J. Glauber, Phys. Rev. 160 (1967) 1097.
[7] D.F. Walls, J. Milburn, Quantum Optics, Springer-Verlag, Berlin, 1994;
M.O. Scully, M.S. Zubairy, Quantum Optics, Cambridge University Press, Cambridge, 1997.
[8] S. Schneider, G.J. Milburn, Phys. Rev. A 57 (1998) 3748;
Phys. Rev. A 59 (1999) 3766.
[9] C. Di Fidio, W. Vogel, Phys. Rev. A 62 (2000) 031802(R).
[10] R.M. Serra, N.G. de Almeida, W.B. da Costa, M.H.Y. Moussa, Phys. Rev. A 64 (2001) 033419.
[11] A.A. Budini, R.L. de Matos, N. Zagury, J. Opt. B: Quantum Semiclass. Opt. 4 (2002) S462.
[12] J.I. Cirac, P. Zoller, H.J. Kimble, H. Mabuchi, Phys. Rev. Lett. 78 (1997) 3221;
T. Pellizzari, Phys. Rev. Lett. 79 (1997) 5242;
H.J. Briegel, W. Dür, J.I. Cirac, P. Zoller, Phys. Rev. Lett. 81 (1998) 5932;
S.J. van Enk, H.J. Kimble, J.I. Cirac, P. Zoller, Phys. Rev. A 59 (1999) 2659.
[13] P. Shor, in: S. Goldwasser (Ed.), Proceedings of the 35th Annual Symposium on the Theory of Computer Science, IEEE Computer Society Press, Los Alamitos, CA, 1994, p. 124;
P. Shor, in: Goldwasser, S. (Ed.), Proceedings of the 35th Annual Symposium on the Theory of Computer Science, IEEE Computer Society Press, Los Alamitos, CA, p. 124. Available from: <quant-ph/9508027>;
J.I. Cirac, P. Zoller, Phys. Rev. Lett. 74 (1995) 4091;
Q.A. Turchette, C.J. Hood, W. Lange, H. Mabuchi, H.J. Kimble, Phys. Rev. Lett. 75 (1995) 4710;
I.L. Chuang, L.M.K. Vandersypen, X. Zhou, D.W. Leung, S. Lloyd, Nature 393 (1998) 143;
B.E. Kane, Nature 393 (1998) 143;
L.M.K. Vandersypen, M. Steffen, G. Breyta, C.S. Yannoni, M.H. Sherwood, I.L. Chuang, Nature 414 (2001) 883.
[14] M.A. Nielsen, I.L. Chuang, Quantum Computation and Quantum Information, Cambridge University Press, UK, 2000.
[15] M.C. de Oliveira, W.J. Munro, Phys. Rev. A 61 (2000) 42309.
[16] S. Haroche, Phys. Today 51 (7) (1998) 36.
[17] D. Vitali, P. Tombesi, Phys. Rev. A 59 (1999) 4178.
[18] D. Vitali, P. Tombesi, G.J. Milburn, Phys. Rev. Lett. 79 (1997) 2442;
J. Mod. Opt. 44 (1997) 2033.
[19] M.C. de Oliveira, M.H.Y. Moussa, S.S. Mizrahi, Phys. Rev. A 61 (2000) 63809;
J. Opt B: Quantum Semiclass. Opt. 3 (2001) 57.
[20] J.F. Poyatos, J.I. Cirac, P. Zoller, Phys. Rev. Lett. 77 (1996) 4728.
[21] C.J. Myatt, B.E. King, Q.A. Turchette, C.A. Sackett, D. Kielpinski, W.M. Itano, C. Monroe, D.J. Wineland, Nature 403 (2000) 269.
[22] A.R.R. Carvalho, P. Milman, R.L. deMatosFilho, L. Davidovich, Phys. Rev. Lett. 86 (2001) 4988.
[23] A.M. Steane, Phys. Rev. A 68 (2003) 042322.
[24] M.S. Byrd, Lian-Ao Wu, D.A. Lidar. Availabel from: <quant-ph/0402098>.
[25] J.M. Raimond, M. Brune, S. Haroche, Phys. Rev. Lett. 79 (1997) 1964.
[26] J. Steinbach, J. Twamley, P.L. Knight, Phys. Rev. A 56 (1997) 4815.
[27] D.J. Wineland, C. Monroe, W.M. Itano, D. Leibfried, B.E. King, D.M. Meekhof, J. Res. NIST 103 (1998) 259.
[28] P.M. Platzman, M.I. Dykman, Science 284 (1999) 1967.
[29] A.J. Dahm, J.M. Goodkind, I. Karakurt, S. Pilla, J. Low Temp. Phys. 126 (2002) 709.
[30] N. Studart, S.S. Sokolov, in: E.Y Andrei (Ed.), Two-Dimensional Electron System, Kluwer Academic Publishers, Netherlands, 1997.
[31] D.F. Walls, Z. Physik 234 (1970) 231.

[32] H.J Carmichael, D.F. Walls, Phys. A 6 (1973) 1552.
[33] S.G. Mokarzel, A.N. Salgueiro, M.C. Nemes, Phys. Rev. A 65 (2002) 044101.
[34] H. Zoubi, M. Orenstien, A. Ron, Phys. Rev. A 62 (2000) 033801.
[35] M.A. de Ponte, M.C. de Oliveira, M.H.Y. Moussa, Phys. Rev. A 70 (2004) 022324;
M.A. de Ponte, M.C. de Oliveira, M.H.Y. Moussa, Phys. Rev. A 70 (2004) 022325.
[36] M. Koashi, A. Winter, Phys. Rev. A 69 (2004) 022309.
[37] M.H.Y. Moussa, S.S. Mizrahi, A.O. Caldeira, Phys. Lett. A 221 (1996) 145.
[38] M.C. de Oliveira, S.S. Mizrahi, V.V. Dodonov, J. Opt. B 1 (1999) 610.
[39] G.W. Ford, J.T. Lewis, R.F. O'Connell, Phys. Rev. A 37 (1988) 4419;
G.W. Ford, R.F. O'Connell, Phys. A 37 (1997) 377.
[40] M. Rosenau da Costa, A.O. Caldeira, S.M. Dutra, H. Westfahl Jr., Phys. Rev. A 61 (2000) 022107.
[41] B.E. King, C.S. Wood, C.J. Myatt, Q.A. Turchette, D. Leibfried, W.M. Itano, C. Monroe, D.J. Wineland, Phys. Rev. Lett. 81 (1998) 1525.
[42] A.J. Leggett, S. Chakravarty, A.T. Dorsey, M.P.A. Fisher, A. Garg, W. Zwerger, Rev. Mod. Phys. 59 (1987) 1.
[43] R.J. Glauber, Phys. Rev. 131 (1963) 2766.
[44] E.C.G. Sudarshan, Phys. Rev. Lett. 10 (1963) 277.
[45] G.J. Milburn, A.S. Lane, D.F. Walls, Phys. Rev. A 27 (1983) 2804.
[46] C.W. Gardiner, P. Zoller, Quantum Noise: A Handbook of Markovian and Non-Markovian Quantum Stochastic Methods with Applications to Quantum Optics, Springer, Berlin, 2000.
[47] P. Bocchieri, A. Loinger, Phys. Rev. 107 (1957) 337.
[48] P.W. Shor, in: Proceedings of the 35th Annual Symposium on the Foundations of Computer Science. Los Amitos, CA, IEEE Computer Society press, NY, 1994.